

# Big Bang Nucleosynthesis: Probing the First 20 Minutes

GARY STEIGMAN

*Departments of Physics and of Astronomy, The Ohio State University*

---

## Abstract

Within the first 20 minutes of the evolution of the hot, dense, early Universe, astrophysically interesting abundances of deuterium, helium-3, helium-4, and lithium-7 were synthesized by the cosmic nuclear reactor. The primordial abundances of these light nuclides produced during Big Bang Nucleosynthesis (BBN) are sensitive to the universal density of baryons and to the early-Universe expansion rate which at early epochs is governed by the energy density in relativistic particles (“radiation”) such as photons and neutrinos. Some 380 kyr later, when the cosmic background radiation (CBR) radiation was freed from the embrace of the ionized plasma of protons and electrons, the spectrum of temperature fluctuations imprinted on the CBR also depended on the baryon and radiation densities. The comparison between the constraints imposed by BBN and those from the CBR reveals a remarkably consistent picture of the Universe at two widely separated epochs in its evolution. Combining these two probes leads to new and tighter constraints on the baryon density at present, on possible new physics beyond the standard model of particle physics, as well as identifying some challenges to astronomy and astrophysics. In this review the current status of BBN will be presented along with the associated estimates of the baryon density and of the energy density in radiation.

## 1.1 Introduction

The present Universe is observed to be expanding and filled with radiation (the 2.7 K cosmic background radiation; CBR) as well as with “ordinary matter” (baryons), “dark matter,” and “dark energy.” As a consequence, the early Universe must have been hot and dense. Sufficiently early in its evolution, the universal energy density would have been dominated by relativistic particles (“radiation dominated”). During its early evolution the Universe passed through a brief epoch when it functioned as a cosmic nuclear reactor, synthesizing the lightest nuclides: D,  $^3\text{He}$ ,  $^4\text{He}$ , and  $^7\text{Li}$ . These relics from the distant past provide a unique window on the early evolution of the Universe, as well as being valuable probes of the standard models of cosmology and particle physics. Comparing the predicted primordial abundances with those inferred from observational data tests the standard models and may uncover clues to their modifications and/or to extensions beyond them. It is clear that Big Bang Nucleosynthesis (BBN), one of the pillars of modern cosmology, has a crucial role to play as the study of the evolution of the Universe enters a new, data-rich era.

As with all science, cosmology depends on the interplay between theoretical ideas and

*G. Steigman*

observational data. As new and better data become available, models may need to be refined, revised, or even replaced. A consequence of this is that any *review* such as this one is merely a signpost along the road to a better understanding of our Universe. While details of the current “standard” model, along with some of its more popular variants to be discussed here, may need to be revised or rejected in the future, the underlying physics to be described here can provide a useful framework and context for understanding those changes. Any quantitative conclusions to be reached today will surely need to be modified in the light of new data. This review is, then, a status report on the standard model, highlighting its successes as well as exposing the current challenges it faces. While we may rejoice in the consistency of the standard model, there is still much work, theoretical and observational, to be done.

## 1.2 An Overview of BBN

To set a context for the confrontation of theoretical predictions with observational data it is useful to review the physics and cosmology of the early evolution of the Universe, touching on the specifics relevant for the synthesis of the light nuclides during the first  $\sim 20$  minutes. In this section is presented an overview of this evolution along with the predicted primordial abundances, first in the standard model and then for two examples of nonstandard models which involve variations on the early-Universe expansion rate (Steigman, Schramm, & Gunn 1977) or asymmetries between the number of neutrinos and antineutrinos (e.g., Kang & Steigman 1992, and references therein).

### 1.2.1 Early Evolution

Discussion of BBN can begin when the Universe is a few tenths of a second old and the temperature is a few MeV. At such an early epoch the energy density is dominated by the relativistic (R) particles present, and the Universe is said to be “radiation-dominated.” For sufficiently early times, when the temperature is a few times higher than the electron rest-mass energy, these are photons,  $e^\pm$  pairs, and, for the standard model of particle physics, three flavors of left-handed (i.e., one helicity state) neutrinos (and their right-handed antineutrinos).

$$\rho_R = \rho_\gamma + \rho_e + 3\rho_\nu = \frac{43}{8}\rho_\gamma, \quad (1.1)$$

where  $\rho_\gamma$  is the energy density in CBR photons (which, today, have redshifted to become the CBR photons at a temperature of 2.7 K).

In standard BBN (SBBN) it is assumed that the neutrinos are fully decoupled prior to  $e^\pm$  annihilation and do not share in the energy transferred from the annihilating  $e^\pm$  pairs to the CBR photons. In this approximation, in the post- $e^\pm$  annihilation Universe, the photons are hotter than the neutrinos by a factor  $T_\gamma/T_\nu = (11/4)^{1/3}$ , and the relativistic energy density is

$$\rho_R = \rho_\gamma + 3\rho_\nu = 1.68\rho_\gamma. \quad (1.2)$$

During these radiation-dominated epochs the age ( $t$ ) and the energy density are related by  $\frac{32\pi G}{3}\rho_R t^2 = 1$ , so that once the particle content ( $\rho_R$ ) is specified, the age of the Universe is known (as a function of the CBR temperature  $T_\gamma$ ). In the standard model,

$$\text{Pre-}e^\pm \text{ annihilation : } t T_\gamma^2 = 0.738 \text{ MeV}^2 \text{ s}, \quad (1.3)$$

G. Steigman

$$\text{Post-}e^\pm \text{ annihilation : } t T_\gamma^2 = 1.32 \text{ MeV}^2 \text{ s.} \quad (1.4)$$

Also present at these early times are neutrons and protons, albeit in trace amounts compared to the relativistic particles. The relative abundance of neutrons and protons is determined by the charged-current weak interactions.

$$p + e^- \longleftrightarrow n + \nu_e, \quad n + e^+ \longleftrightarrow p + \bar{\nu}_e, \quad n \longleftrightarrow p + e^- + \bar{\nu}_e. \quad (1.5)$$

As time goes by and the Universe expands and cools, the lighter protons are favored over the heavier neutrons and the neutron-to-proton ratio decreases, initially following the equilibrium form  $(n/p)_{eq} \propto \exp(-\Delta m/T)$ , where  $\Delta m = 1.29 \text{ MeV}$  is the neutron-proton mass difference. As the temperature drops the two-body collisions in Equation 1.5 become too slow to maintain equilibrium and the neutron-to-proton ratio, while continuing to decrease, begins to deviate from (*exceeds*) this equilibrium value. For later reference, we note that if there is an *asymmetry* between the numbers of  $\nu_e$  and  $\bar{\nu}_e$  (“neutrino degeneracy”), described by a chemical potential  $\mu_e$  (such that for  $\mu_e > 0$  there are more  $\nu_e$  than  $\bar{\nu}_e$ ), then the equilibrium neutron-to-proton ratio is modified to  $(n/p) \propto \exp(-\Delta m/T - \mu_e/T)$ . In place of the neutrino chemical potential, it is convenient to introduce the dimensionless degeneracy parameter  $\xi_e \equiv \mu_e/T$ , which is invariant as the Universe expands.

Prior to  $e^\pm$  annihilation, at  $T \approx 0.8 \text{ MeV}$  when the Universe is  $\sim 1$  second old, the two-body reactions regulating  $n/p$  become slow compared to the universal expansion rate and this ratio “freezes in,” although, in reality, it continues to decrease, albeit more slowly than would be the case for equilibrium. Later, when the Universe is several hundred seconds old, a time comparable to the neutron lifetime ( $\tau_n = 885.7 \pm 0.8 \text{ s}$ ), the  $n/p$  ratio resumes falling exponentially:  $n/p \propto \exp(-t/\tau_n)$ . Since there are several billion CBR photons for every nucleon (baryon), the abundances of any complex nuclei are entirely negligible at these early times.

Notice that since the  $n/p$  ratio depends on the competition between the weak interaction rates and the early-Universe expansion rate (as well as on a possible neutrino asymmetry), any deviations from the standard model (e.g.,  $\rho_R \rightarrow \rho_R + \rho_X$  or  $\xi_e \neq 0$ ) will change the relative numbers of neutrons and protons available for building more complex nuclides.

### 1.2.2 Building the Elements

At the same time that neutrons and protons are interconverting, they are also colliding among themselves to create deuterons:  $n + p \longleftrightarrow D + \gamma$ . However, at early times, when the density and average energy of the CBR photons are very high, the newly formed deuterons find themselves bathed in a background of high-energy gamma rays capable of photodissociating them. Since there are more than a billion photons for every nucleon in the Universe, before the deuteron can capture a neutron or a proton to begin building the heavier nuclides, the deuteron is photodissociated. This bottleneck to BBN persists until the temperature drops sufficiently so that there are too few photons energetic enough to photodissociate the deuterons before they can capture nucleons to launch BBN. This occurs after  $e^\pm$  annihilation, when the Universe is a few minutes old and the temperature has dropped below  $80 \text{ keV}$  ( $0.08 \text{ MeV}$ ).

Once BBN begins in earnest, neutrons and protons quickly combine to form D,  $^3\text{H}$ ,  $^3\text{He}$ , and  $^4\text{He}$ . Here, at  $^4\text{He}$ , there is a different kind of bottleneck. There are no stable mass-5 nuclides. To jump this gap requires  $^4\text{He}$  reactions with D or  $^3\text{H}$  or  $^3\text{He}$ , all of which are

*G. Steigman*

positively charged. The Coulomb repulsion among these colliding nuclei suppresses the reaction rates, ensuring that virtually all of the neutrons available for BBN are incorporated in  $^4\text{He}$  (the most tightly bound of the light nuclides), and also that the abundances of the heavier nuclides are severely depressed below that of  $^4\text{He}$  (and even of D and  $^3\text{He}$ ). Recall that  $^3\text{H}$  is unstable, decaying to  $^3\text{He}$ . The few reactions that manage to bridge the mass-5 gap lead mainly to mass-7 ( $^7\text{Li}$  or  $^7\text{Be}$ , which, later, when the Universe has cooled further, will capture an electron and decay to  $^7\text{Li}$ ); the abundance of  $^6\text{Li}$  is 1 to 2 orders of magnitude below that of the more tightly bound  $^7\text{Li}$ . Finally, there is another gap at mass-8. This absence of any stable mass-8 nuclei ensures there will be no astrophysically interesting production of any heavier nuclides.

The primordial nuclear reactor is short-lived, quickly encountering an energy crisis. Because of the falling temperature and the Coulomb barriers, nuclear reactions cease rather abruptly as the temperature drops below  $\sim 30$  keV, when the Universe is  $\sim 20$  minutes old. This results in “nuclear freeze-out,” since no already existing nuclides are destroyed (except for those that are unstable and decay) and no new nuclides are created. In  $\sim 1000$  seconds BBN has run its course.

### 1.2.3 The SBBN-predicted Abundances

The primordial abundances of D,  $^3\text{He}$ , and  $^7\text{Li}$  ( $^7\text{Be}$ ) are rate limited, depending sensitively on the competition between the nuclear reaction rates (proportional to the nucleon density) and the universal expansion rate. As a result, these nuclides are all potential baryometers. As the Universe expands, the nucleon density decreases so it is useful to compare it to that of the CBR photons:  $\eta \equiv n_{\text{N}}/n_{\gamma}$ . Since this ratio turns out to be very small, it is convenient to introduce

$$\eta_{10} \equiv 10^{10}(n_{\text{N}}/n_{\gamma}) = 274\Omega_{\text{b}}h^2, \quad (1.6)$$

where  $\Omega_{\text{b}}$  is the ratio of the present values of the baryon and critical densities and  $h$  is the present value of the Hubble parameter in units of  $100 \text{ km s}^{-1} \text{ Mpc}^{-1}$ . As the Universe evolves (post- $e^{\pm}$  annihilation) this ratio is accurately preserved so that  $\eta$  at the time of BBN should be equal to its value today. Testing this relation over ten orders of magnitude in redshift, over a timespan of some 10 billion years, can provide a confirmation of, or pose a challenge to the standard model.

In contrast to the other light nuclides, the primordial abundance of  $^4\text{He}$  (mass fraction  $Y$ ) is relatively insensitive to the baryon density, but since virtually all neutrons available at BBN are incorporated in  $^4\text{He}$ ,  $Y$  does depend on the competition between the weak interaction rates (largely fixed by the accurately measured neutron lifetime) and the universal expansion rate. The higher the nucleon density, the earlier can the D bottleneck be breached. Since at early times there are more neutrons (as a fraction of the nucleons), more  $^4\text{He}$  will be synthesized. This latter effect is responsible for a very slow (logarithmic) increase in  $Y$  with  $\eta$ . Given the standard model relation between time and temperature and the measured nuclear and weak cross sections and decay rates, the evolution of the light-nuclide abundances may be calculated and the relic, primordial abundances predicted as a function of the one free parameter, the nucleon density or  $\eta$ . These predictions for SBBN are shown in Figure 1.1.

Not shown on Figure 1.1 are the relic abundances of  $^6\text{Li}$ ,  $^9\text{Be}$ ,  $^{10}\text{B}$ , and  $^{11}\text{B}$ ; for the same range in  $\eta$ , all of them lie offscale, in the range  $10^{-20} - 10^{-13}$ . The results shown here are

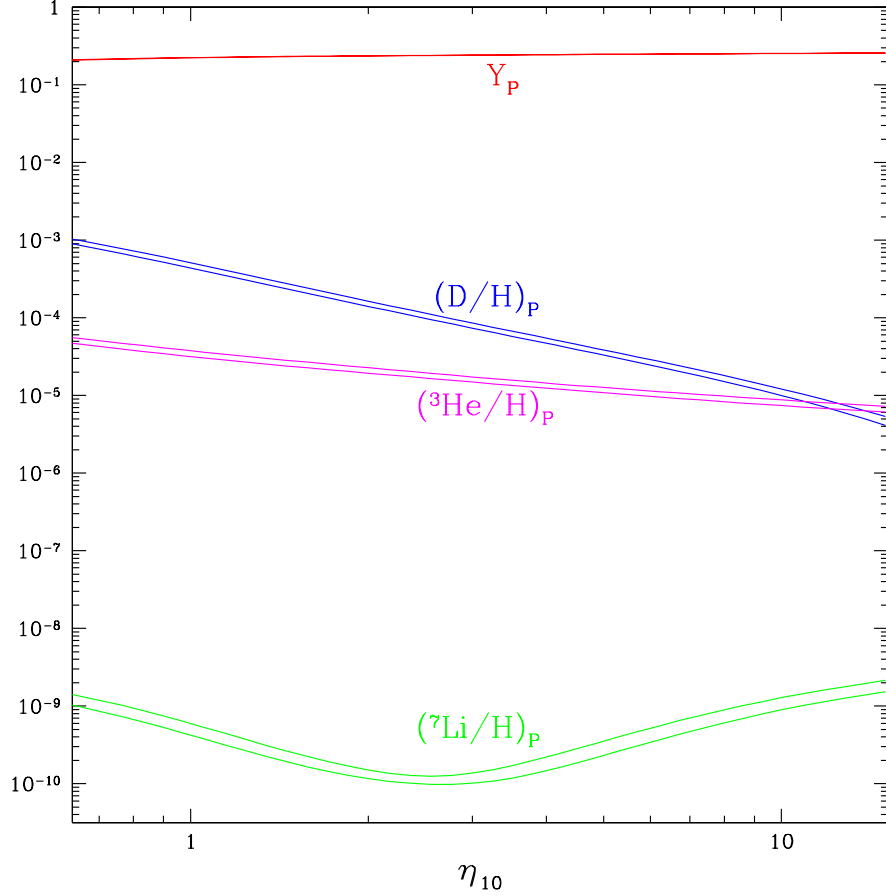


Fig. 1.1. The SBBN-predicted primordial abundances of D,  ${}^3\text{He}$ , and  ${}^7\text{Li}$  (by number with respect to hydrogen), and the  ${}^4\text{He}$  mass fraction  $Y$  as a function of the nucleon abundance  $\eta_{10}$ . The widths of the bands reflect the theoretical uncertainties.

from the BBN code developed and refined over the years by my colleagues at The Ohio State University (OSU). They are in excellent agreement with the published results of the Chicago group (Burles, Nollett, & Turner 2001). Notice that the abundances appear in Figure 1.1 as bands. These reflect the theoretical uncertainties in the predicted abundances. For the OSU code the errors in  $D/H$  and  ${}^3\text{He}/H$  are at the  $\sim 8\%$  level, while they are much larger,  $\sim 12\%$ , for  ${}^7\text{Li}$ . Burles et al. (2001), in a reanalysis of the relevant published cross sections, have reduced the theoretical errors by roughly a factor of 3 for D and  ${}^3\text{He}$  and a factor of 2 for  ${}^7\text{Li}$ . The reader may not notice the band shown for  ${}^4\text{He}$ , since the uncertainty in  $Y$ , dominated by the very small uncertainty in the neutron lifetime, is at only the  $\sim 0.2\%$  level ( $\sigma_Y \approx 0.0005$ ).

Based on the discussion above it is easy to understand the trends shown in Figure 1.1. D and  ${}^3\text{He}$  are burned to  ${}^4\text{He}$ . The higher the nucleon density, the faster this occurs, leaving

*G. Steigman*

behind fewer nuclei of D or  $^3\text{He}$ . The very slight increase of  $Y$  with  $\eta$  is largely due to BBN starting earlier at higher nucleon density (more complete burning of D,  $^3\text{H}$ , and  $^3\text{He}$  to  $^4\text{He}$ ) and higher neutron-to-proton ratio (more neutrons, more  $^4\text{He}$ ). The behavior of  $^7\text{Li}$  is more interesting. At relatively low values of  $\eta_{10} \lesssim 3$ , mass-7 is largely synthesized as  $^7\text{Li}$  [by  $^3\text{H}(\alpha, \gamma)^7\text{Li}$  reactions], which is easily destroyed in collisions with protons. So, as  $\eta$  increases at low values, destruction is faster and  $^7\text{Li}/\text{H}$  *decreases*. In contrast, at relatively high values of  $\eta_{10} \gtrsim 3$ , mass-7 is largely synthesized as  $^7\text{Be}$  [via  $^3\text{He}(\alpha, \gamma)^7\text{Be}$  reactions], which is more tightly bound than  $^7\text{Li}$  and, therefore, harder to destroy. As  $\eta$  increases at high values, the abundance of  $^7\text{Be}$  *increases*. Later in the evolution of the Universe, when it is cooler and neutral atoms begin to form,  $^7\text{Be}$  will capture an electron and  $\beta$ -decay to  $^7\text{Li}$ .

#### 1.2.4 Nonstandard BBN

The predictions of the primordial abundance of  $^4\text{He}$  depend sensitively on the early expansion rate (the Hubble parameter  $H$ ) and on the amount—if any—of a  $\nu_e - \bar{\nu}_e$  asymmetry (the  $\nu_e$  chemical potential  $\mu_e$  or the neutrino degeneracy parameter  $\xi_e$ ). In contrast to  $^4\text{He}$ , the BBN-predicted abundances of D,  $^3\text{He}$  and  $^7\text{Li}$  are determined by the competition between the various two-body production/destruction rates and the universal expansion rate. As a result, the D,  $^3\text{He}$ , and  $^7\text{Li}$  abundances are sensitive to the post- $e^\pm$  annihilation expansion rate, while that of  $^4\text{He}$  depends on *both* the pre- and post- $e^\pm$  annihilation expansion rates; the former determines the “freeze-in” and the latter modulates the importance of  $\beta$ -decay (see, e.g., Kneller & Steigman 2003). Also, the primordial abundances of D,  $^3\text{He}$ , and  $^7\text{Li}$ , while not entirely insensitive to neutrino degeneracy, are much less affected by a nonzero  $\xi_e$  (e.g., Kang & Steigman 1992). Each of these nonstandard cases will be considered below. Note that the abundances of at least two different relic nuclei are needed to break the degeneracy between the baryon density and a possible nonstandard expansion rate resulting from new physics or cosmology, and/or a neutrino asymmetry.

##### 1.2.4.1 Additional Relativistic Energy Density

The most straightforward variation of SBBN is to consider the effect of a nonstandard expansion rate  $H' \neq H$ . To quantify the deviation from the standard model it is convenient to introduce the “*expansion rate factor*” (or speedup/slowdown factor)  $S$ , where

$$S \equiv H'/H = t/t'. \quad (1.7)$$

Such a nonstandard expansion rate might result from the presence of “extra” energy contributed by new, light (relativistic at BBN) particles “ $X$ ”. These might, but need not, be additional flavors of active or sterile neutrinos. For  $X$  particles that are decoupled, in the sense that they do not share in the energy released by  $e^\pm$  annihilation, it is convenient to account for the extra contribution to the standard-model energy density by normalizing it to that of an “equivalent” neutrino flavor (Steigman et al. 1977),

$$\rho_X \equiv \Delta N_\nu \rho_\nu = \frac{7}{8} \Delta N_\nu \rho_\gamma. \quad (1.8)$$

For SBBN,  $\Delta N_\nu = 0$  ( $N_\nu \equiv 3 + \Delta N_\nu$ ) and for each such additional “neutrino-like” particle (i.e., any two-component fermion), if  $T_X = T_\nu$ , then  $\Delta N_\nu = 1$ ; if  $X$  should be a scalar,  $\Delta N_\nu = 4/7$ . However, it may well be that the  $X$  have decoupled even earlier in the evolution of the Universe and have failed to profit from the heating when various other particle-antiparticle

*G. Steigman*

pairs annihilated (or unstable particles decayed). In this case, the contribution to  $\Delta N_\nu$  from each such particle will be  $< 1$  ( $< 4/7$ ). Henceforth we drop the  $X$  subscript. Note that, in principle, we are considering any term in the energy density that scales like “radiation” (i.e., decreases with the expansion of the Universe as the fourth power of the scale factor). In this sense, the modification to the usual Friedman equation due to higher dimensional effects, as in the Randall-Sundrum model (Randall & Sundrum 1999a,b; see also Cline, Grojean, & Servant 1999; Binetruy et al. 2000; Bratt et al. 2002), may be included as well. The interest in this latter case is that it permits the possibility of an apparent *negative* contribution to the radiation density ( $\Delta N_\nu < 0$ ;  $S < 1$ ). For such a modification to the energy density, the pre- $e^\pm$  annihilation energy density in Equation 1.1 is changed to

$$(\rho_R)_{pre} = \frac{43}{8} \left( 1 + \frac{7\Delta N_\nu}{43} \right) \rho_\gamma. \quad (1.9)$$

Since any *extra* energy density ( $\Delta N_\nu > 0$ ) speeds up the expansion of the Universe ( $S > 1$ ), the right-hand side of the time-temperature relation in Equation 1.3 is smaller by the square root of the factor in parentheses in Equation 1.9.

$$S_{pre} \equiv (t/t')_{pre} = \left( 1 + \frac{7\Delta N_\nu}{43} \right)^{1/2} = (1 + 0.163\Delta N_\nu)^{1/2}. \quad (1.10)$$

In the post- $e^\pm$  annihilation Universe the extra energy density is diluted by the heating of the photons, so that

$$(\rho_R)_{post} = 1.68(1 + 0.135\Delta N_\nu)\rho_\gamma \quad (1.11)$$

and

$$S_{post} \equiv (t/t')_{post} = (1 + 0.135\Delta N_\nu)^{1/2}. \quad (1.12)$$

While the abundances of D,  $^3\text{He}$ , and  $^7\text{Li}$  are most sensitive to the baryon density ( $\eta$ ), the  $^4\text{He}$  mass fraction ( $Y$ ) provides the best probe of the expansion rate. This is illustrated in Figure 1.2 where, in the  $\Delta N_\nu - \eta_{10}$  plane, are shown isoabundance contours for D/H and  $Y_P$  (the isoabundance curves for  $^3\text{He}/\text{H}$  and for  $^7\text{Li}/\text{H}$ , omitted for clarity, are similar in behavior to that of D/H). The trends illustrated in Figure 1.2 are easy to understand in the context of the discussion above. The higher the baryon density ( $\eta_{10}$ ), the faster primordial D is destroyed, so the relic abundance of D is *anticorrelated* with  $\eta_{10}$ . But, the faster the Universe expands ( $\Delta N_\nu > 0$ ), the less time is available for D destruction, so D/H is positively, albeit weakly, correlated with  $\Delta N_\nu$ . In contrast to D (and to  $^3\text{He}$  and  $^7\text{Li}$ ), since the incorporation of all available neutrons into  $^4\text{He}$  is not limited by the nuclear reaction rates, the  $^4\text{He}$  mass fraction is relatively insensitive to the baryon density, but it is very sensitive to both the pre- and post- $e^\pm$  annihilation expansion rates (which control the neutron-to-proton ratio). The faster the Universe expands, the more neutrons are available for  $^4\text{He}$ . The very slow increase of  $Y_P$  with  $\eta_{10}$  is a reflection of the fact that for a higher baryon density, BBN begins earlier, when there are more neutrons. As a result of these complementary correlations, the pair of primordial abundances  $y_D \equiv 10^5(\text{D}/\text{H})_P$  and  $Y_P$ , the  $^4\text{He}$  mass fraction, provide observational constraints on both the baryon density ( $\eta$ ) and on the universal expansion rate factor  $S$  (or on  $\Delta N_\nu$ ) when the Universe was some 20 minutes old. Comparing these to similar constraints from when the Universe was some 380 Kyr old, provided by the *WMAP* observations of the CBR polarization and the spectrum of temperature fluctuations, provides

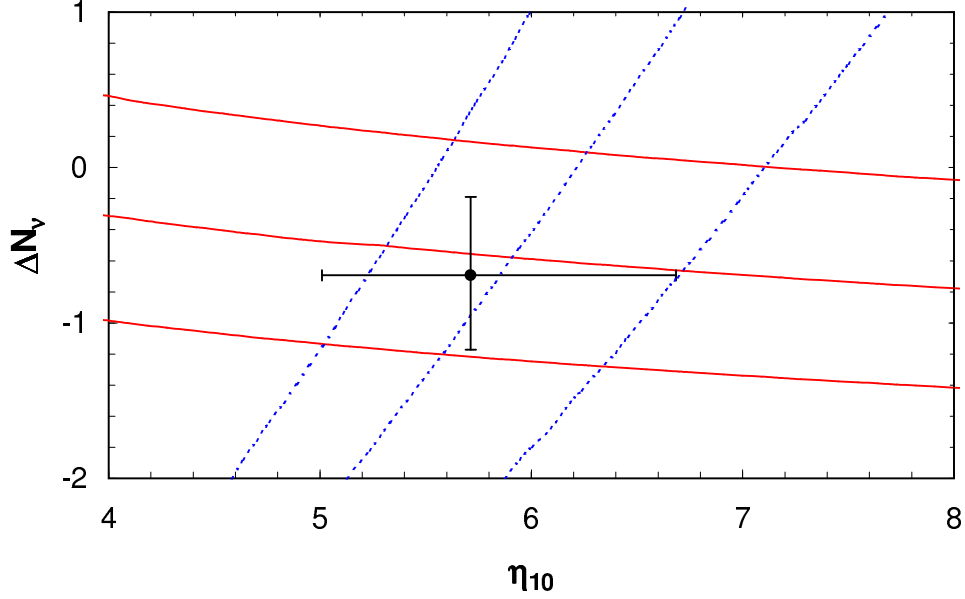


Fig. 1.2. Isoabundance curves for D and  ${}^4\text{He}$  in the  $\Delta N_\nu - \eta_{10}$  plane. The solid curves are for  ${}^4\text{He}$  (from top to bottom:  $Y = 0.25, 0.24, 0.23$ ). The dotted curves are for D (from left to right:  $y_D \equiv 10^5(\text{D}/\text{H}) = 3.0, 2.5, 2.0$ ). The data point with error bars corresponds to  $y_D = 2.6 \pm 0.4$  and  $Y_p = 0.238 \pm 0.005$ ; see the text for discussion of these abundances.

a test of the consistency of the standard models of cosmology and of particle physics and further constrains the allowed range of the present-Universe baryon density (e.g., Barger et al. 2003a,b; Crotty, Lesgourgues, & Pastor 2003; Hannestad 2003; Pierpaoli 2003).

#### 1.2.4.2 Neutrino Degeneracy

The baryon-to-photon ratio provides a dimensionless measure of the universal baryon asymmetry, which is very small ( $\eta \lesssim 10^{-9}$ ). By charge neutrality the asymmetry in the charged leptons must also be of this order. However, there are no observational constraints, save those to be discussed here (see Kang & Steigman 1992; Kneller et al. 2002, and further references therein), on the magnitude of any asymmetry among the neutral leptons (neutrinos). A relatively small asymmetry between electron type neutrinos and antineutrinos ( $\xi_e \gtrsim 10^{-2}$ ) can have a significant impact on the early-Universe ratio of neutrons to protons, thereby affecting the yields of the light nuclides formed during BBN. The strongest effect is on the BBN  ${}^4\text{He}$  abundance, which is neutron limited. For  $\xi_e > 0$ , there is an excess of neutrinos ( $\nu_e$ ) over antineutrinos ( $\bar{\nu}_e$ ), and the two-body reactions regulating the neutron-to-proton ratio (Eq. 1.5) drive down the neutron abundance; the reverse is true for  $\xi_e < 0$ . The effect of a nonzero  $\nu_e$  asymmetry on the relic abundances of the other light nuclides is much weaker. This is illustrated in Figure 1.3, which shows the D and  ${}^4\text{He}$  isoabundance curves in the  $\xi_e - \eta_{10}$  plane. The nearly horizontal  ${}^4\text{He}$  curves reflect the weak dependence of  $Y_p$  on the baryon density, along with its significant dependence on the neutrino asymmetry. In contrast, the nearly vertical D curves reveal the strong dependence of  $y_D$  on the baryon density



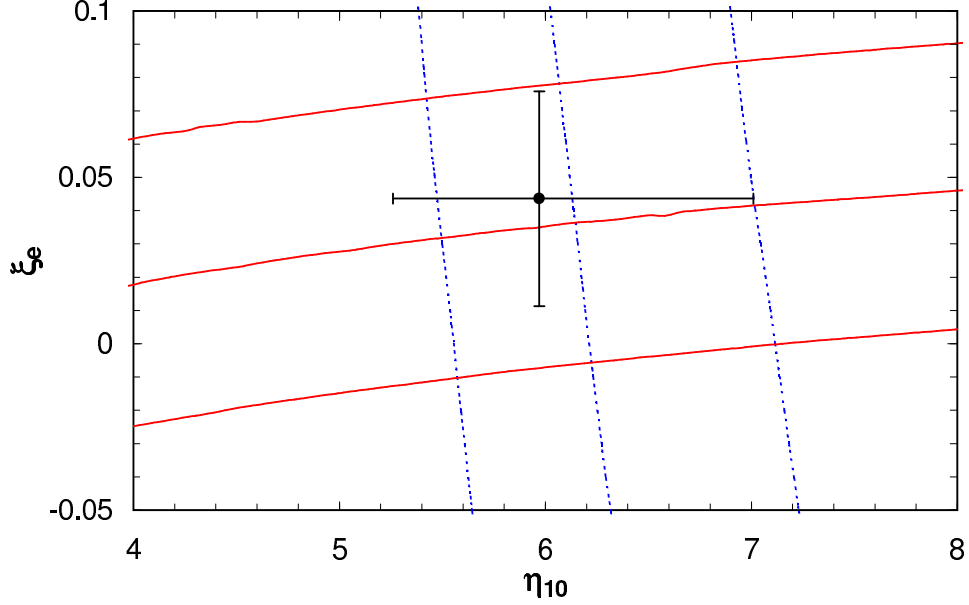


Fig. 1.3. Isoabundance curves for D and  $^4\text{He}$  in the  $\xi_e - \eta_{10}$  plane. The solid curves are for  $^4\text{He}$  (from top to bottom:  $Y_p = 0.23, 0.24, 0.25$ ). The dotted curves are for D (from left to right:  $y_D \equiv 10^5(\text{D}/\text{H}) = 3.0, 2.5, 2.0$ ). The data point with error bars corresponds to  $y_D = 2.6 \pm 0.4$  and  $Y_p = 0.238 \pm 0.005$ ; see the text for discussion of these abundances.

and its weak dependence on any neutrino asymmetry ( $^3\text{He}/\text{H}$  and  $^7\text{Li}/\text{H}$  behave similarly: strongly dependent on  $\eta$ , weakly dependent on  $\xi_e$ ). This complementarity between  $y_D$  and  $Y_p$  permits the pair  $\{\eta, \xi_e\}$  to be determined once the primordial abundances of D and  $^4\text{He}$  are inferred from the appropriate observational data.

### 1.3 Primordial Abundances

It is clear from Figures 1.1 – 1.3 that tests of the consistency of SBBN, along with constraints on any new physics, will be data-driven. While D (and/or  $^3\text{He}$  and/or  $^7\text{Li}$ ) largely constrain the baryon density and  $^4\text{He}$  plays a similar role for  $\Delta N_\nu$  and/or for  $\xi_e$ , there is an interplay among  $\eta_{10}$ ,  $\Delta N_\nu$ , and  $\xi_e$ , which is quite sensitive to the adopted abundances. For example, a *lower* primordial D/H *increases* the BBN-inferred value of  $\eta_{10}$ , leading to a *higher* predicted primordial  $^4\text{He}$  mass fraction. If the primordial  $^4\text{He}$  mass fraction derived from the data is “low,” then a low upper bound on  $\Delta N_\nu$  (or a nonzero lower bound on  $\xi_e$ ) will be inferred. It is therefore crucial to avoid biasing any conclusions by *underestimating* the present uncertainties in the primordial abundances derived from the observational data.

The four light nuclides of interest, D,  $^3\text{He}$ ,  $^4\text{He}$ , and  $^7\text{Li}$  follow very different evolutionary paths in the post-BBN Universe. In addition, the observations leading to their abundance determinations are also very different. Neutral D is observed in absorption in the UV; singly ionized  $^3\text{He}$  is observed in emission in Galactic H II regions; both singly and doubly ionized  $^4\text{He}$  are observed in emission via recombinations in extragalactic H II regions;  $^7\text{Li}$  is observed in absorption in the atmospheres of very metal-poor halo stars. The different histories and

*G. Steigman*

observational strategies provide some insurance that systematic errors affecting the inferred primordial abundances of any one of the light nuclides are unlikely to distort the inferred abundances of the others.

### **1.3.1 Deuterium**

The post-BBN evolution of D is straightforward. As gas is incorporated into stars the very loosely bound deuteron is burned to  $^3\text{He}$  (and beyond). Any D that passes through a star is destroyed. Furthermore, there are no astrophysical sites where D can be produced in an abundance anywhere near that observed (Epstein, Lattimer, & Schramm 1976). As a result, as the Universe evolves and gas is cycled through generations of stars, deuterium is only destroyed. Therefore, observations of the deuterium abundance anywhere, anytime, provide *lower* bounds on its primordial abundance. Furthermore, if D can be observed in “young” systems, in the sense of very little stellar processing, the observed abundance should be very close to the primordial value. Thus, while there are extensive data on deuterium in the solar system and the local interstellar medium of the Galaxy, it is the handful of observations of deuterium absorption in high-redshift, low-metallicity QSO absorption-line systems (QSOALS), which are potentially the most valuable. At sufficiently high redshifts and low metallicities, the primordial abundance of deuterium should reveal itself as a “deuterium plateau.”

Inferring the primordial D abundance from the QSOALS has not been without its difficulties, with some abundance claims having been withdrawn or revised. Presently there are  $\sim$  half a dozen QSOALS with reasonably firm deuterium detections (Burles & Tytler 1998a,b; D’Odorico, Dessauges-Zavadsky, & Molaro 2001; O’Meara et al. 2001; Pettini & Bowen 2002; Kirkman et al. 2004). However, there is significant dispersion among the derived abundances, and the data fail to reveal the anticipated deuterium plateau (Fig. 1.4 – 1.6; see also Steigman 2004). Furthermore, subsequent observations of the D’Odorico et al. (2001) QSOALS by Levshakov et al. (2002) revealed a more complex velocity structure and led to a revised—and uncertain—deuterium abundance. This sensitivity to poorly constrained velocity structure in the absorbers is also exposed in the analyses of published QSOALS data by Levshakov and collaborators (Levshakov, Kegel, & Takahara 1998a,b, 1999), which lead to consistent, but somewhat higher, deuterium abundances than those inferred from “standard” data reduction analyses.

Indeed, the absorption spectra of D I and H I are identical, except for a wavelength/velocity offset resulting from the heavier reduced mass of the deuterium atom. An H I “interloper,” a low-column density cloud shifted by  $\sim 81 \text{ km s}^{-1}$  with respect to the main absorbing cloud, would masquerade as D I. If this is not accounted for, a D/H ratio which is too high would be inferred. Since there are more low-column density absorbers than those with high H I column densities, absorption-line systems with somewhat lower H I column density (e.g., Lyman-limit systems) are more susceptible to this contamination than are the higher H I column density absorbers (e.g., damped Ly $\alpha$  absorbers). However, for the damped Ly $\alpha$  absorbers, an accurate determination of the H I column density requires an accurate placement of the continuum, which could be compromised by interlopers. This might lead to an overestimate of the H I column density and a concomitant underestimate of D/H (J. Linsky, private communication). As will be seen, there is the possibility that each of these effects may have contaminated the current data. Indeed, complex velocity structure in the D’Odorico et al. (2001) absorber (see Levshakov et al. 2002) renders it of less value in

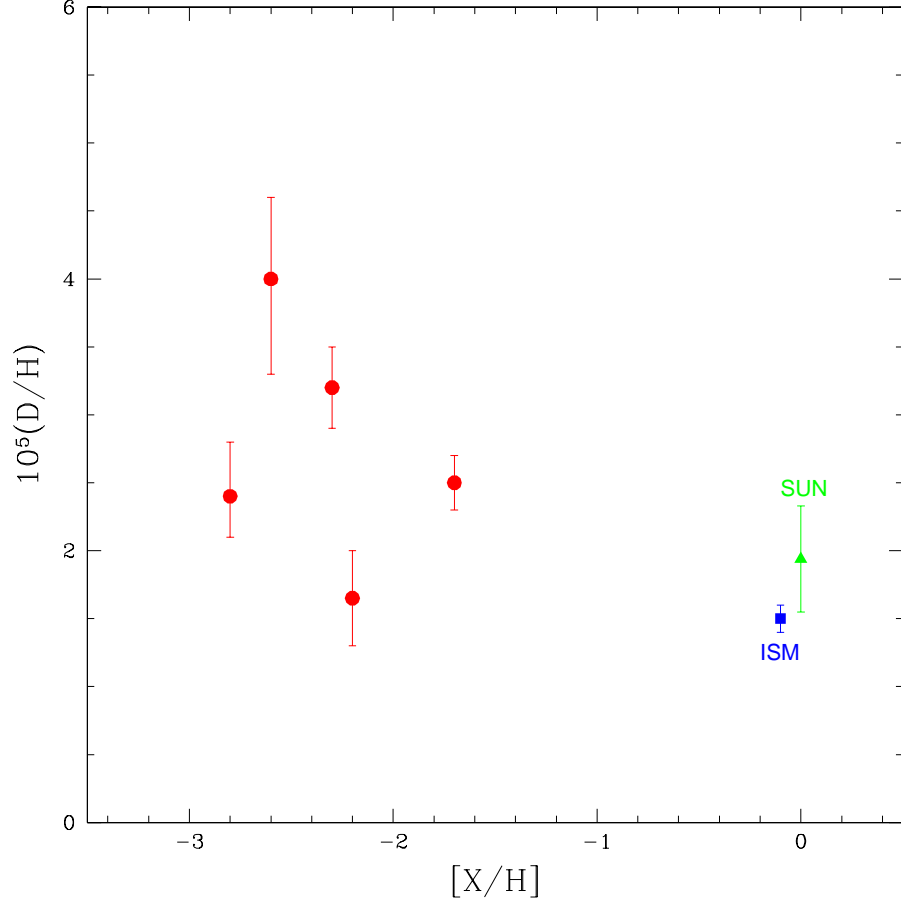


Fig. 1.4. The deuterium abundance,  $D/H$ , versus metallicity, “X”(usually,  $X = \text{Si}$ ), from observations (as of early 2003) of QSOALS (filled circles). Also shown for comparison are the  $D$  abundances for the local ISM (filled square) and the solar system (“Sun”; filled triangle).

constraining primordial deuterium, and it will not be included in the estimates presented here.

In Figure 1.4 are shown the extant data (circa June 2003) for  $D/H$  as a function of metallicity from the work of Burles & Tytler (1998a,b), O’Meara et al. (2001), Pettini & Bowen (2002), and Kirkman et al. (2004). Also shown for comparison are the local interstellar medium (ISM)  $D/H$  (Linsky & Wood 2000) and that for the presolar nebula as inferred from solar system data (Geiss & Gloeckler 1998).

On the basis of our discussion of the post-BBN evolution of  $D/H$ , a “deuterium plateau” at low metallicity was expected. If, indeed, one is present, it is hidden by the dispersion in the current data. Given the possibility that interlopers may affect both the  $D\text{ I}$  and the  $\text{H I}$  column

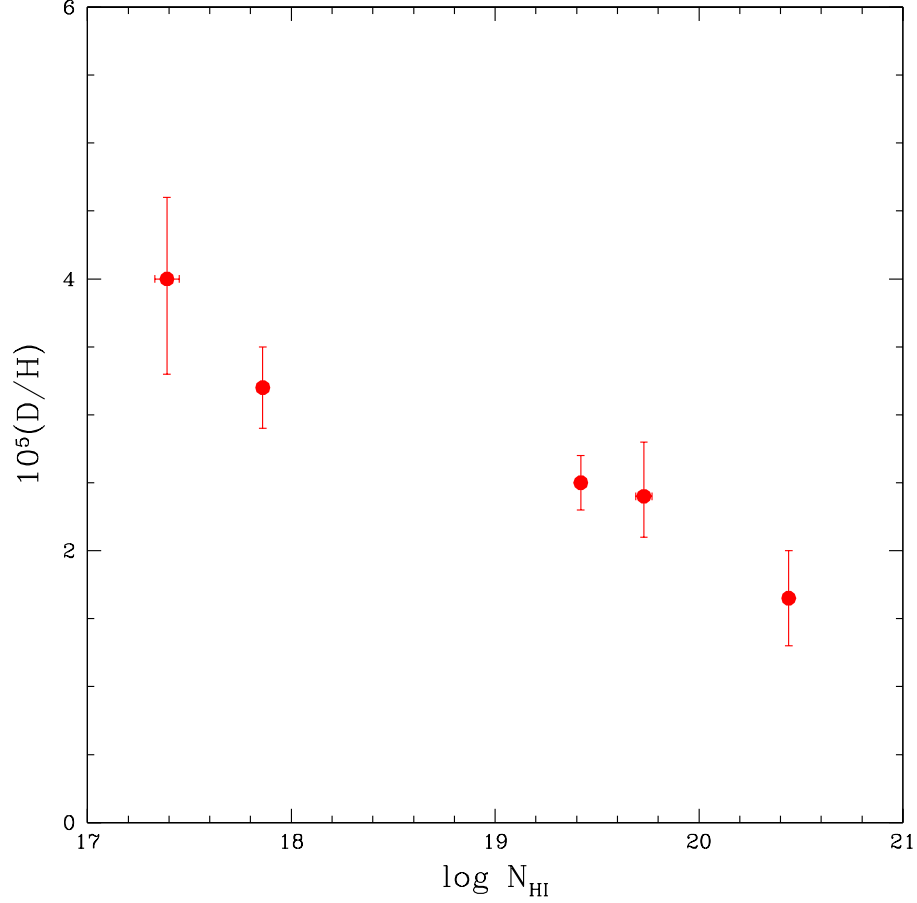


Fig. 1.5. The deuterium abundance,  $D/H$ , versus the  $H\text{I}$  column density in the absorbers,  $N(H\text{I})$ , for the same QSOALS as in Figure 1.4.

density determinations, it is interesting to plot  $D/H$  as a function of  $N(H\text{I})$ . This is shown in Figure 1.5, where there is some (limited) evidence that  $D/H$  is higher in the Lyman-limit systems than in the damped  $\text{Ly}\alpha$  absorbers.

To decide how to utilize this confusing data it may be of value to consider the observations chronologically. Of the set chosen here, Burles & Tytler (1998a,b) studied the first two lines of sight. For PKS 1937–1009 they derived  $y_D \equiv 10^5(D/H) = 3.25 \pm 0.3$  (Burles & Tytler 1998a), while for Q1009+299 they found  $y_D = 3.98^{+0.59}_{-0.67}$  (Burles & Tytler 1998b). These two determinations are in excellent agreement with each other ( $\chi^2 = 1.0$ ), leading to a mean abundance  $\langle y_D \rangle = 3.37 \pm 0.27$ . Next, O’Meara et al. (2001) added the line of sight to HS 0105+1619, finding a considerably lower abundance  $y_D = 2.54 \pm 0.23$ . Indeed, while the weighted mean for these three lines of sight is  $\langle y_D \rangle = 2.88$ , the  $\chi^2$  has ballooned to 6.4 (for two degrees of freedom). Absent any evidence that one or more of

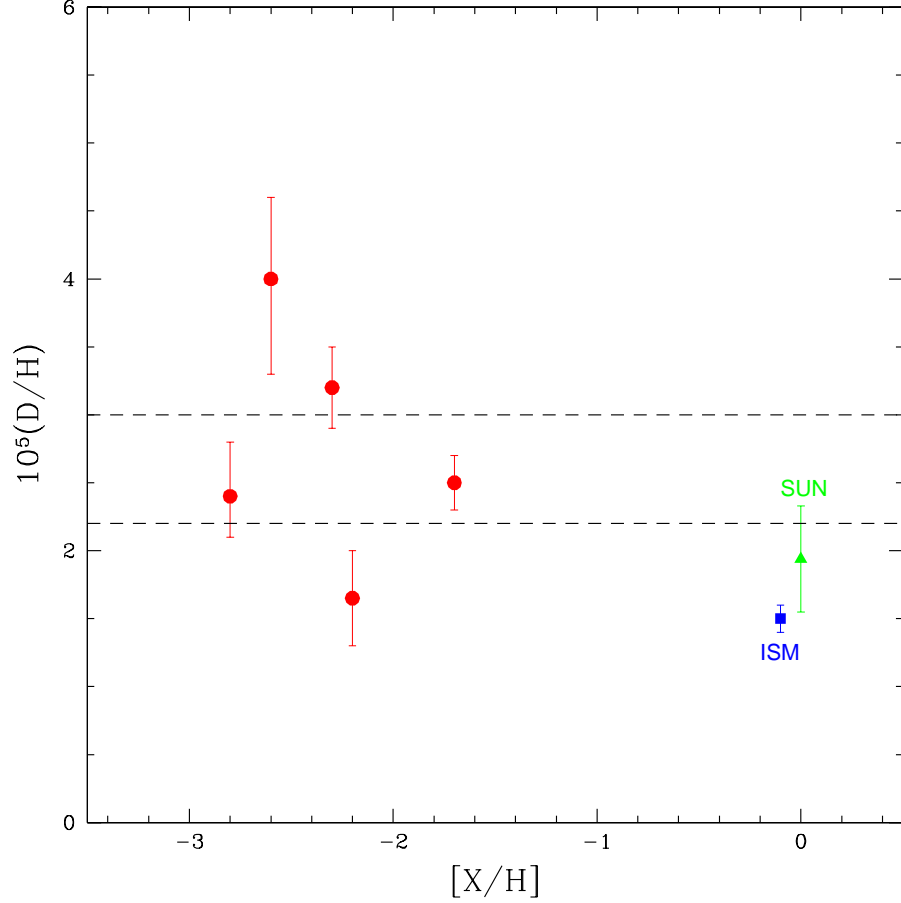


Fig. 1.6. As in Figure 1.4. The dashed lines represent the  $\pm 1\sigma$  band calculated from the mean and its dispersion ( $(D/H)_P = 2.6 \pm 0.4 \times 10^{-5}$ ; see the text).

these abundances is in error, O’Meara et al. adopt the mean, and, for the error in the mean, they take the dispersion about the mean (0.72) divided by the square root of the number of data points:  $\langle y_D \rangle = 2.88 \pm 0.42$ . One year later Pettini & Bowen (2002) published their *HST* data on the line of sight toward Q2206–199, finding a surprisingly low value of  $y_D = 1.65 \pm 0.35$ . Including this determination reduces the mean to  $\langle y_D \rangle = 2.63$ , but the dispersion in  $y_D$  grows to 1.00 and  $\chi^2 = 16.3$  for three degrees of freedom. Clearly, either one or more of these determinations is in error, or the variation among the high-redshift, low-metallicity deuterium abundances is larger than anticipated from our understanding of its evolution (Jedamzik & Fuller 1997). Using the mean and its dispersion (to fix the error), as of the time of the Carnegie Symposium, the best estimate for the primordial D abundance was  $\langle y_D \rangle = 2.63 \pm 0.50$ . Shortly thereafter, in early 2003, the data of Kirkman et al. (2004) appeared for the line of sight toward Q1243+3047. For this line of sight they find  $y_D =$

*G. Steigman*

$2.42^{+0.35}_{-0.25}$ . This abundance lies between the lowest and the higher previous values, reducing the overall dispersion to 0.88, while hardly changing the mean from  $y_D = 2.63$  to 2.60. While the total  $\chi^2$  is still enormous, increasing slightly to 16.6, the reduced  $\chi^2$  decreases from 5.4 to 4.2. This is still far too large, suggesting that one or more of these determinations may be contaminated, or that there may actually be real variations in D/H at high redshifts and low metallicities. Notice (see Fig. 1.5) that the largest D/H estimates are from the two absorbers with the lowest H I column densities (Lyman-limit systems), where interlopers *might* contribute to the inferred D I column densities, while the lowest abundances are from the higher H I column density (damped Ly $\alpha$ ) absorbers, where interlopers *might* affect the wings of the H I lines used to fix the H I column densities. Absent any further data supporting, or refuting, these possibilities, there is no *a priori* reason to reject any of these determinations.

To utilize the current data, the weighted mean D abundances for these five lines of sight and the dispersion are used to infer the abundance of primordial deuterium (and its uncertainty) adopted in this review:  $y_D = 2.6 \pm 0.4$ . Note that, given the large dispersion, two-decimal place accuracy seems to be wishful thinking at present. For this reason, in quoting the primordial D abundance inferred from the observational data I have purposely chosen to quote values to only one decimal place. This choice is consistent too with the  $\sim 3\% - 8\%$  theoretical uncertainty (at fixed  $\eta$ ) in the BBN-predicted abundance. In Figure 1.6 are shown the data, along with the corresponding  $1\sigma$  band. It is worth remarking that using the same data Kirkman et al. (2004) derive a slightly higher mean D abundance:  $y_D = 2.74$ . The reason for the difference is that they first find the mean of  $\log(y_D)$  and then use it to compute the mean D abundance ( $y_D \equiv 10^{(\log(y_D))}$ ).

### 1.3.2 Helium-3

The post-BBN evolution of  $^3\text{He}$  is considerably more complex and model dependent than that of D. Interstellar  $^3\text{He}$  incorporated into stars is burned to  $^4\text{He}$  (and beyond) in the hotter interiors, but preserved in the cooler, outer layers. Furthermore, while hydrogen burning in cooler, low-mass stars is a net producer of  $^3\text{He}$  (Iben 1967; Rood 1972; Dearborn, Schramm, & Steigman 1986; Vassiliadis & Wood 1993; Dearborn, Steigman, & Tosi 1996) it is unclear how much of this newly synthesized  $^3\text{He}$  is returned to the interstellar medium and how much of it is consumed in post-main sequence evolution (e.g., Sackmann & Boothroyd 1999a,b). Indeed, it is clear that when the data (Geiss & Gloeckler 1998; Rood et al. 1998; Bania, Rood, & Balser 2002) are compared to a large variety of chemical evolution models (Rood, Steigman, & Tinsley 1976; Dearborn et al. 1996; Galli et al. 1997; Palla et al. 2000; Chiappini, Renda, & Matteucci 2002), agreement is only possible for a very delicate balance between net production and net destruction of  $^3\text{He}$ . For a recent review of the current status of  $^3\text{He}$  evolution, see Romano et al. (2004). Given this state of affairs it is not possible to utilize  $^3\text{He}$  as a baryometer, but it may perhaps be used to provide a consistency check. To this end, the abundance inferred by Bania et al. (2002) from an H II region in the outer Galaxy, where post-BBN evolution might have been minimal, is adopted here:  $y_3 \equiv 10^5(^3\text{He}/\text{H}) = 1.1 \pm 0.2$ .

### 1.3.3 Helium-4

Helium-4 is the second most abundant nuclide in the Universe after hydrogen. In post-BBN evolution gas cycling through stars has its hydrogen burned to helium, increasing the  $^4\text{He}$  abundance above its primordial value. As with deuterium, a  $^4\text{He}$  “plateau” is ex-

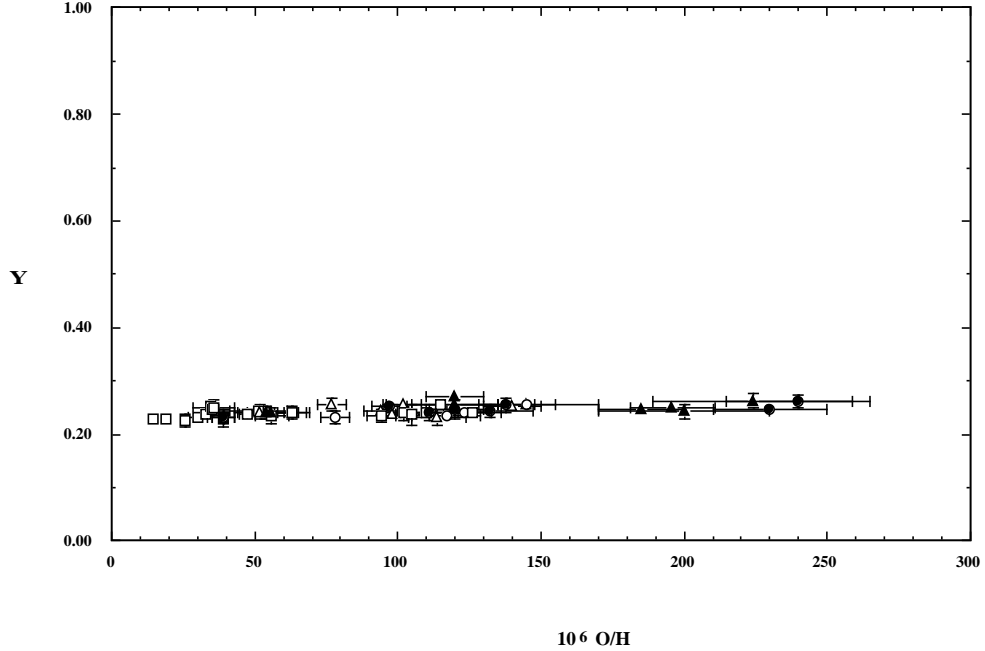


Fig. 1.7. The  ${}^4\text{He}$  mass fraction,  $Y$ , inferred from observations of low-metallicity, extragalactic H II regions versus the oxygen abundance derived from the same data. (Figure courtesy of K. A. Olive.)

pected at sufficiently low metallicity. Although  ${}^4\text{He}$  is observed in the Sun and in Galactic H II regions, the crucial data for inferring its primordial abundance is from observations of the helium and hydrogen emission (recombination) lines from low-metallicity, extragalactic H II regions. The present inventory of such regions studied for their helium content is approaching of order 100. Thus, it is not surprising that even with modest observational errors for any individual H II region, the statistical uncertainty in the inferred primordial abundance may be quite small. In this situation, care must be taken with hitherto ignored or unaccounted for corrections and systematic errors or biases.

In Figure 1.7 is shown a compilation of the data used by Olive & Steigman (1995) and Olive, Skillman, & Steigman (1997), along with the independent data set obtained by Izotov, Thuan, & Lipovetsky (1997) and Izotov & Thuan (1998). To track the evolution of the  ${}^4\text{He}$  mass fraction,  $Y$  is plotted versus the H II region oxygen abundance. These H II regions are all metal poor, ranging from  $\sim 1/2$  down to  $\sim 1/40$  of solar (for a solar oxygen abundance of  $\text{O}/\text{H} \approx 5 \times 10^{-4}$ ; Allende-Prieto, Lambert, & Asplund 2001). A key feature of Figure 1.7 is that for sufficiently low metallicity the  $Y$  versus  $\text{O}/\text{H}$  relation approaches a  ${}^4\text{He}$  plateau! Since  $Y$  increases with metallicity, the relic abundance can either be bounded from above by the lowest metallicity regions, or the  $Y$  versus  $\text{O}/\text{H}$  relation may be extrapolated to zero metallicity. The extrapolation is quite small, so that whether the former or the latter approach is adopted the difference in the inferred primordial abundance is small:  $|\Delta Y| \lesssim 0.001$ .

While the data shown in Figure 1.7 reveal a well-defined primordial abundance for  ${}^4\text{He}$ , the scale hides the very small statistical errors as well as the tension between the two

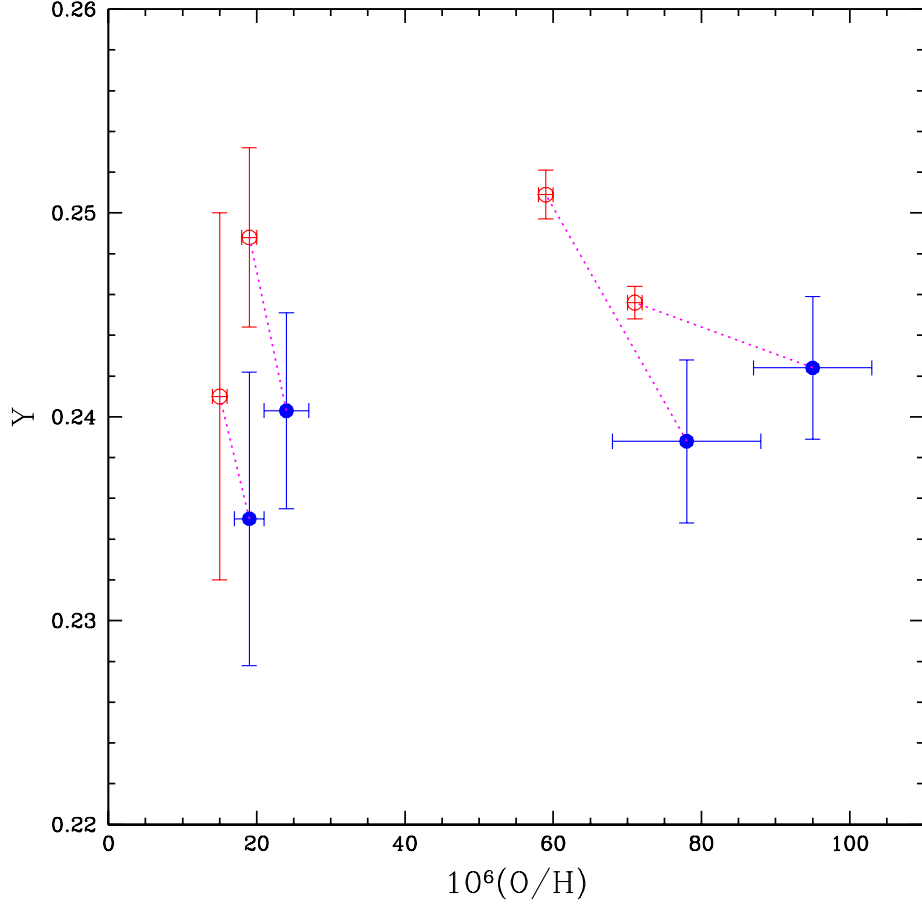


Fig. 1.8. The Peimbert et al. (2002) reanalysis of the  $^4\text{He}$  abundance data for four of the Izotov & Thuan (1998) H II regions. The open circles are the Izotov & Thuan (1998) abundances, while the filled circles are from Peimbert et al. (2002).

groups' helium abundances. Olive & Steigman (1995) and Olive et al. (1997) find  $Y_p = 0.234 \pm 0.003$ , but Izotov et al. (1997) and Izotov & Thuan (1998) derive  $Y_p = 0.244 \pm 0.002$ . Although it is difficult to account for all of the difference, much of it is traceable to the different ways the two groups correct for the contribution to the emission lines from collisional excitation of neutral helium and also to Izotov and collaborators rejecting some helium emission lines *a posteriori* when they yield “too low” an abundance. Furthermore, for either data set, there are additional corrections for temperature, for temperature and density fluctuations, and for ionization, which when applied can change the inferred primordial  $^4\text{He}$  abundance by more than the quoted statistical errors (see, e.g., Steigman, Viegas, & Gruenwald 1997; Viegas, Gruenwald, & Steigman 2000; Gruenwald, Steigman, & Viegas 2002; Peimbert, Peimbert & Luridiana 2002; Sauer & Jedamzik 2002).



*G. Steigman*

For example, Peimbert et al. (2002) recently reanalyzed the data from four of the Izotov & Thuan (1998) H II regions, employing their own H II region temperatures and accounting for temperature fluctuations. Peimbert et al. (2002) derive systematically lower helium abundances, as shown in Figure 1.8. From this very limited sample Peimbert et al. suggest that the Izotov & Thuan (1998) estimate for the primordial  $^4\text{He}$  mass fraction might have to be reduced by as much as  $\sim 0.007$ . Peimbert et al. go further, combining their redetermined helium abundances for these four H II regions with an accurate determination of  $Y$  in a more metal-rich H II region (Peimbert, Peimbert, & Ruiz 2000). Although these five data points are consistent with zero slope in the  $Y - \text{O}/\text{H}$  relation, leading to a primordial abundance  $Y_{\text{P}} = 0.240 \pm 0.001$ , this extremely small data set is also consistent with  $\Delta Y \approx 40(\text{O}/\text{H})$ , leading to a smaller primordial estimate of  $Y_{\text{P}} \approx 0.237$ .

It seems clear that until new data address the unresolved systematic errors afflicting the derivation of the primordial helium abundance, the true errors must be much larger than the statistical uncertainties. In an attempt to account for this, here I follow Olive, Steigman, & Walker (2000) and adopt a compromise mean value along with a larger uncertainty:  $Y_{\text{P}} = 0.238 \pm 0.005$ .

#### **1.3.4 Lithium-7**

Lithium-7 is fragile, burning in stars at a relatively low temperature. As a result, the majority of any interstellar  $^7\text{Li}$  cycled through stars is destroyed. For the same reason, it is difficult for stars to create new  $^7\text{Li}$  and/or to return any newly synthesized  $^7\text{Li}$  to the ISM before it is destroyed by nuclear burning. In addition to synthesis in stars, the intermediate-mass nuclides  $^6\text{Li}$ ,  $^7\text{Li}$ ,  $^9\text{Be}$ ,  $^{10}\text{B}$ , and  $^{11}\text{B}$  can be synthesized via cosmic ray nucleosynthesis, either by alpha-alpha fusion reactions, or by spallation reactions (nuclear breakup) in collisions between protons and alpha particles and CNO nuclei. In the early Galaxy, when the metallicity is low, the post-BBN production of lithium is expected to be subdominant to that from BBN abundance. As the data in Figure 1.9 reveal, only relatively late in the evolution of the Galaxy does the lithium abundance increase. The data also confirm the anticipated “Spite plateau” (Spite & Spite 1982), the absence of a significant slope in the  $\text{Li}/\text{H}$  versus  $[\text{Fe}/\text{H}]$  relation at low metallicity due to the dominance of BBN-produced  $^7\text{Li}$ . The plateau is a clear signal of the primordial lithium abundance. Notice, also, the enormous *spread* among the lithium abundances at higher metallicity. This range in  $\text{Li}/\text{H}$  likely results from the destruction/dilution of lithium on the surfaces of the observed stars while they are on the main sequence and/or lithium destruction during their pre-main sequence evolution, implying that it is the *upper envelope* of the  $\text{Li}/\text{H}$  versus  $[\text{Fe}/\text{H}]$  relation that preserves the history of Galactic lithium evolution. Note, also, that at low metallicity the dispersion is much narrower, suggesting that corrections for depletion/dilution are (may be) much smaller for the Population II stars.

As with the other relic nuclides, the dominant uncertainties in estimating the primordial abundance of  $^7\text{Li}$  are not statistical, but systematic. The lithium observed in the atmospheres of cool, metal-poor, Population II halo stars is most relevant for determining the BBN  $^7\text{Li}$  abundance. Uncertainties in the lithium equivalent width measurements, in the temperature scales for the cool Population II stars, and in their model atmospheres dominate the overall error budget. For example, Ryan et al. (2000), using the Ryan, Norris, & Beers (1999) data, infer  $[\text{Li}]_{\text{P}} \equiv 12 + \log(\text{Li}/\text{H}) = 2.1$ , while Bonifacio & Molaro (1997) and Bonifacio, Molaro, & Pasquini (1997) derive  $[\text{Li}]_{\text{P}} = 2.2$ , and Thorburn (1994) finds  $[\text{Li}]_{\text{P}} = 2.3$ . From

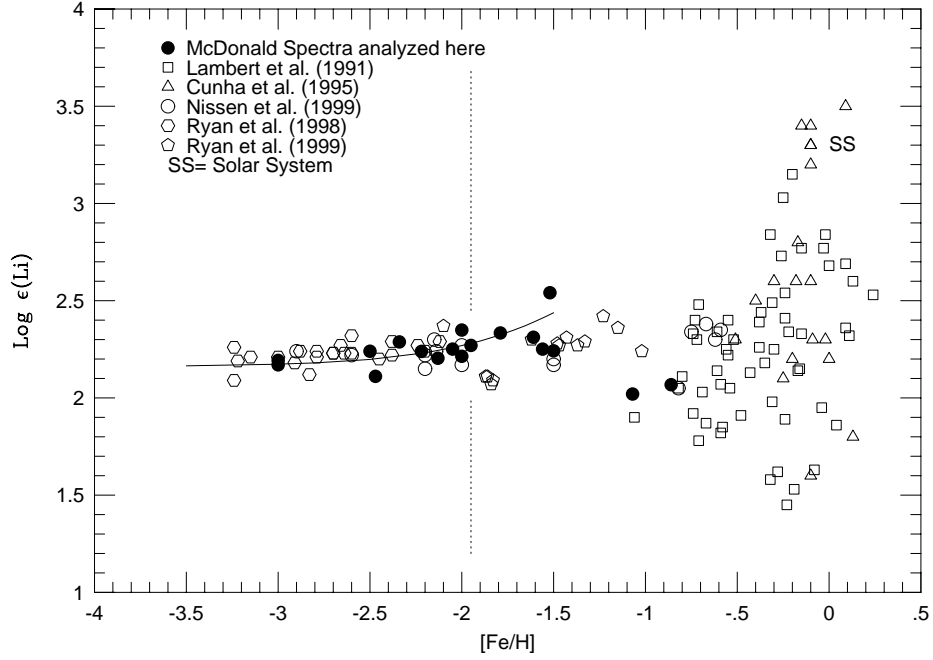


Fig. 1.9. A compilation of the lithium abundance data as a function of metallicity from stellar observations (courtesy of V. V. Smith).  $\epsilon(\text{Li}) \equiv 10^{12}(\text{Li}/\text{H})$ , and  $[\text{Fe}/\text{H}]$  is the usual logarithmic metallicity relative to solar. Note the “Spite plateau” in  $\text{Li}/\text{H}$  for  $[\text{Fe}/\text{H}] \lesssim -2$ .

recent observations of stars in a metal-poor globular cluster, Bonifacio et al. (2002) derive  $[\text{Li}]_{\text{p}} = 2.34 \pm 0.056$ . As may be seen from Figure 1.9, the indication from the preliminary data assembled by V. V. Smith (private communication) favors a Spite plateau at  $[\text{Li}]_{\text{p}} \approx 2.2$ .

In addition to these intrinsic uncertainties, there are others associated with stellar structure and evolution. The metal-poor halo stars that define the primordial lithium plateau are very old. As a result, they have had time to disturb the prestellar lithium that could survive in their cooler, outer layers. Mixing of these outer layers with the hotter interior where lithium has been (can be) destroyed will dilute or deplete the surface lithium abundance. Pinsonneault et al. (1999, 2002) have shown that rotational mixing may decrease the surface abundance of lithium in these Population II stars by 0.1 – 0.3 dex while still maintaining the rather narrow *dispersion* among the plateau abundances (see also Chaboyer et al. 1992; Theado & Vauclair 2001; Salaris & Weiss 2002). Pinsonneault et al. (2002) adopted for a baseline (Spite plateau) estimate  $[\text{Li}] = 2.2 \pm 0.1$ , while for an overall depletion factor  $0.2 \pm 0.1$  dex was chosen. Adding these contributions to the log of the primordial lithium abundance *linearly*, an estimate  $[\text{Li}]_{\text{p}} = 2.4 \pm 0.2$  was derived. In the comparison between theory and observation below, I will adopt the Ryan et al. (2000) estimate  $[\text{Li}]_{\text{p}} = 2.1 \pm 0.1$ , but I will also consider the implications of the Pinsonneault et al. (2002) value.

## 1.4 Confrontation of Theory with Data

Having reviewed the basic physics and cosmological evolution underlying BBN and summarized the observational data leading to a set of adopted primordial abundances, the predictions may now be confronted with the data. There are several possible approaches that might be adopted. The following option is chosen here. First, concentrating on the predictions of SBBN, deuterium will be used as the baryometer of choice to fix the baryon-to-photon ratio  $\eta$ . This value and its uncertainty are then used to “predict” the  $^3\text{He}$ ,  $^4\text{He}$ , and  $^7\text{Li}$  abundances, which are compared to those adopted above. This comparison can provide a test of the consistency of SBBN as well as identify those points of “tension” between theory and observation. This confrontation is carried further to consider the two extensions beyond the standard model [ $S \neq 1$  ( $\Delta N_\nu \neq 0$ );  $\xi_e \neq 0$ ].

### 1.4.1 Testing the Standard Model

For SBBN, the baryon density corresponding to the D abundance adopted here ( $y_D = 2.6 \pm 0.4$ ) is  $\eta_{10} = 6.1^{+0.7}_{-0.5}$ , corresponding to  $\Omega_b = 0.022^{+0.003}_{-0.002}$ . This is in outstanding agreement with the estimate of Spergel et al. (2003), based largely on the new CBR (WMAP) data (Bennett et al. 2003):  $\Omega_b = 0.0224 \pm 0.0009$ . For the baryon density determined by D, the SBBN-predicted abundance of  $^3\text{He}$  is  $y_3 = 1.0 \pm 0.1$ , which is to be compared to the outer-Galaxy abundance of  $y_3 = 1.1 \pm 0.1$ , which is suggested by Bania et al. (2002) to be nearly primordial. Again, the agreement is excellent.

The tension between the data and SBBN arises with  $^4\text{He}$ . Given the very slow variation of  $Y_P$  with  $\eta$ , along with the very high accuracy of the SBBN-predicted abundance, the primordial abundance is tightly constrained:  $Y_{\text{SBBN}} = 0.248 \pm 0.001$ . This should be compared with our adopted estimate of  $Y = 0.238 \pm 0.005$  (Olive et al. 2000). Agreement is only at the  $\sim 5\%$  level. This tension is shown in Figure 1.10. This apparent challenge to SBBN is also an opportunity. As already noted, while the  $^4\text{He}$  abundance is insensitive to the baryon density, it is very sensitive to new physics (i.e., nonstandard universal expansion rate and/or neutrino degeneracy).

There is tension, too, when comparing the SBBN-predicted abundance of  $^7\text{Li}$  with the (very uncertain) primordial abundance inferred from the data. For SBBN the expected abundance is  $[\text{Li}]_P = 2.65^{+0.09}_{-0.11}$ . This is to be compared with the various estimates above that suggested  $[\text{Li}]_P \approx 2.2 \pm 0.1$ . In Figure 1.11 is shown the analog of Figure 1.10 for lithium and deuterium. Depending on the assessment of the uncertainty in the primordial abundance inferred from the observational data, the conflict with SBBN may or may not be serious. In contrast to  $^4\text{He}$ ,  $^7\text{Li}$  is more similar to D (and to  $^3\text{He}$ ) in that its BBN-predicted abundance is relatively insensitive to new physics. As a result, this tension, if it persists, could be a signal of interesting new astrophysics (e.g., have the halo stars depleted or diluted their surface lithium?).

### 1.4.2 Nonstandard Expansion Rate: $S \neq 1$ ( $\Delta N_\nu \neq 0$ )

The excellent agreement between the SBBN-predicted baryon density inferred from the primordial-D abundance and that derived from the CBR and large scale structure (Spergel et al. 2003), and also the agreement between predicted and observed D and  $^3\text{He}$  suggest that the tension with  $^4\text{He}$ , if not observational or astrophysical in origin, may be a sign of new physics. As noted earlier,  $Y_P$  is sensitive to the early-Universe expansion rate (while D,  $^3\text{He}$ , and  $^7\text{Li}$  are less so). A faster expansion ( $S > 1$ ,  $\Delta N_\nu > 0$ ) leads to a higher predicted pri-

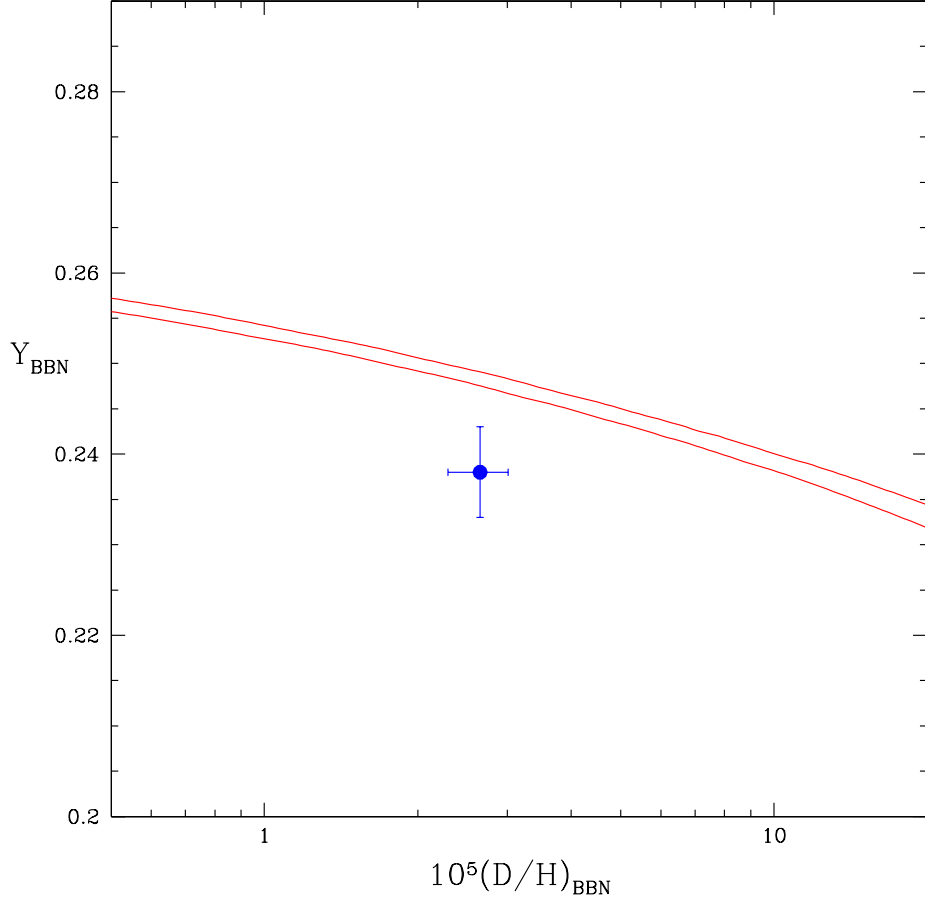


Fig. 1.10. The SBBN-predicted relation between the primordial abundances of D and  ${}^4\text{He}$  (mass fraction) is shown by the band, whose thickness represents the uncertainties in the predicted abundances. Also shown by the point and error bars are the adopted primordial abundances of D and  ${}^4\text{He}$  (see the text).

mordial abundance of  ${}^4\text{He}$ , and *vice versa* for  $S < 1$  ( $\Delta N_\nu < 0$ ). In Figure 1.12 is shown the same  $Y_{\text{P}}$  versus  $y_{\text{D}}$  band as for SBBN in Figure 1.10, along with the corresponding bands for the nonstandard cases of a faster expansion ( $\Delta N_\nu = 4$ ) and a slower expansion ( $\Delta N_\nu = 2$ ). It can be seen that the data “prefer” a slower than standard early-Universe expansion rate. If both  $\eta$  and  $\Delta N_\nu$  are allowed to be free, it is possible (not surprisingly) to accommodate the adopted primordial abundances of D and  ${}^4\text{He}$  (see Fig. 1.2). Given the similar effects of  $\Delta N_\nu \neq 0$  on the BBN-predicted D,  ${}^3\text{He}$ , and  ${}^7\text{Li}$  abundances, while it is possible to maintain the good agreement (from SBBN) for  ${}^3\text{He}$ , the tension between  ${}^7\text{Li}$  and D cannot be relieved. In Figure 1.13 are shown the 1-, 2-, and 3- $\sigma$  BBN contours in the  $\eta - \Delta N_\nu$  plane

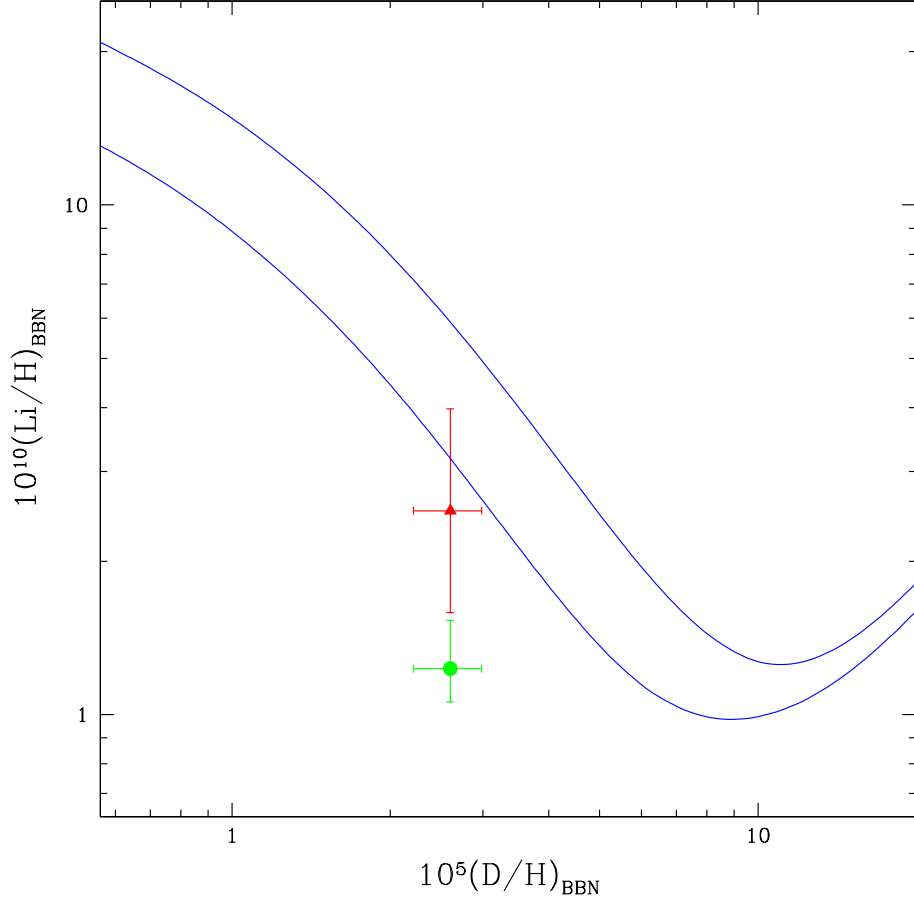


Fig. 1.11. The SBBN-predicted relation between the primordial abundances of D and  ${}^7\text{Li}$  is shown by the band, whose thickness reflects the uncertainties in the predicted abundances. The data points are for the primordial abundance of D adopted here along with the Ryan et al. (2000) Li abundance (filled circle) and the Pinsonneault et al. (2002) Li abundance (filled triangle).

derived from the adopted values of  $y_{\text{D}}$  and  $Y_{\text{P}}$ . Although the best-fit point is at  $\Delta N_{\nu} = -0.7$  (and  $\eta_{10} = 5.7$ ), it is clear that SBBN ( $N_{\nu} = 3$ ) is acceptable.

The CBR temperature anisotropy spectrum and polarization are also sensitive to the early-Universe expansion rate (see, e.g., Barger et al. 2003a, and references therein). There is excellent overlap between the  $\eta - \Delta N_{\nu}$  confidence contours from BBN as shown in Figure 1.13 and from the CBR (Barger et al. 2003a). In Figure 1.14 are shown the confidence contours in the  $\eta - \Delta N_{\nu}$  plane for a joint BBN – CBR fit (Barger et al. 2003a). Again, while the best fit value for  $\Delta N_{\nu}$  is negative (driven largely by the adopted value for  $Y_{\text{P}}$ ),  $\Delta N_{\nu} = 0$  is quite acceptable.

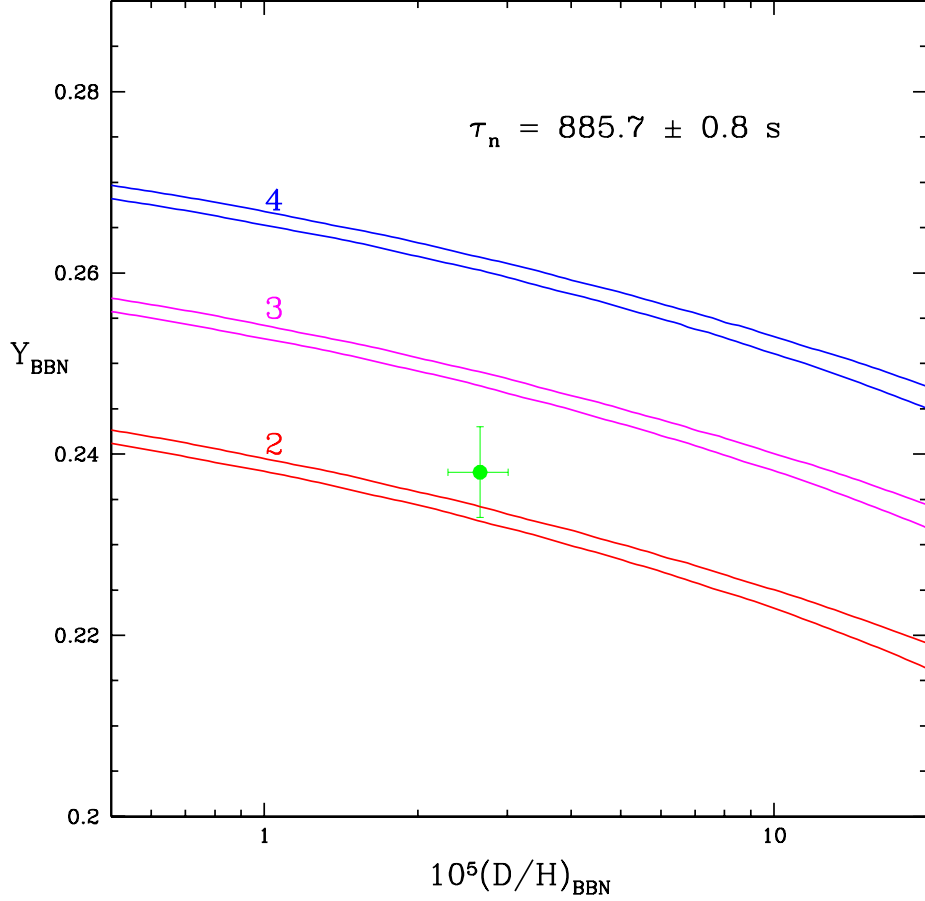


Fig. 1.12. As in Figure 1.10 for  $N_\nu = 2, 3, 4$ , which correspond to  $S = 0.915, 1, 1.078$ .

#### 1.4.3 Neutrino Asymmetry ( $\xi_e \neq 0$ )

The tension between D and  $^4\text{He}$  can also be relieved by nonstandard neutrino physics (see Fig. 1.3). Although the asymmetry (difference between the numbers of particles and antiparticles) in charged leptons, tied to that in the baryons by charge neutrality of the Universe, must be very small, the neutrino asymmetry is unconstrained observationally. Of relevance to BBN is the asymmetry between the electron neutrinos and the electron antineutrinos ( $\xi_e$ ), which regulates the pre-BBN neutron-to-proton ratio through the reactions in Equation 1.5. In Figure 1.15 are shown the 1- and 2- $\sigma$  contours in the  $\eta$ - $\xi_e$  plane for BBN (for  $N_\nu = 3$ ) and the adopted abundances of D and  $^4\text{He}$ . As seen before for  $\Delta N_\nu \neq 0$ , while a fit to the data can be achieved for  $\xi_e \neq 0$ , the data are not inconsistent with  $\xi_e = 0$ . Furthermore, as is shown in Figure 1.15, BBN constrains the allowed range for neutrino asymmetry to be very small. For further implications for neutrino physics and for a discussion of the case where *both*  $\Delta N_\nu$  and  $\xi_e$  are free to differ from zero, see Barger et al. (2003b).

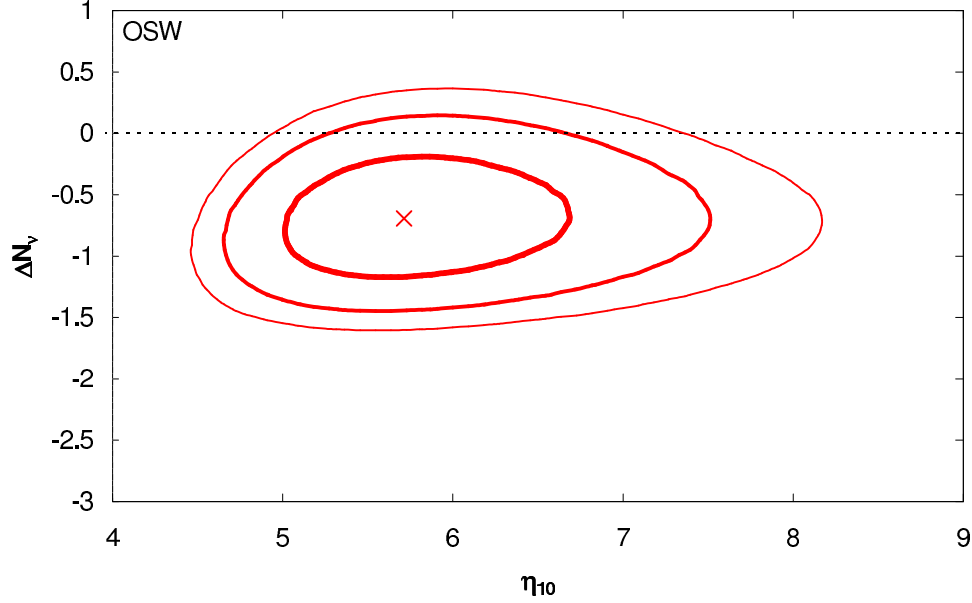


Fig. 1.13. The 1-, 2-, and 3- $\sigma$  contours in the  $\eta - \Delta N_\nu$  plane for BBN and the adopted D and  $^4\text{He}$  abundances.

### 1.5 Summary and Conclusions

Given the standard models of cosmology and particle physics, SBBN predicts the primordial abundances of D,  $^3\text{He}$ ,  $^4\text{He}$ , and  $^7\text{Li}$ , which may be compared with the observational data. Of the light nuclides, deuterium is the baryometer of choice, while  $^4\text{He}$  is an excellent chronometer. The universal density of baryons inferred from SBBN and the adopted primordial D abundance is in excellent (exact!) agreement with that derived from non-BBN, mainly CBR data (Spergel et al. 2003):  $\eta_{10}(\text{SBBN}) = 6.10^{+0.67}_{-0.52}$ ;  $\eta_{10}(\text{CBR}) = 6.14 \pm 0.25$ . For this baryon density, the predicted primordial abundance of  $^3\text{He}$  is also in excellent agreement with the (very uncertain) value inferred from observations of an outer-Galaxy H II region (Bania et al. 2002). In contrast, the SBBN-predicted mass fraction of  $^4\text{He}$  for the concordant baryon density is  $Y_p = 0.248 \pm 0.001$ , while that inferred from observations of recombination lines in metal-poor, extragalactic H II regions is lower (Olive et al. 2000):  $Y_p^{\text{obs}} = 0.238 \pm 0.005$ . Since the uncertainties in the observationally inferred primordial value are likely dominated by systematics, this  $\sim 2\sigma$  difference may not be cause for (much) concern. Finally, there appears to be a more serious issue concerning the predicted and observed lithium abundances. While the predicted abundance is  $[\text{Li}]_p \approx 2.6 \pm 0.1$ , current observations of metal-poor halo stars suggest a considerably smaller value  $\approx 2.2 \pm 0.1$ .

It has been seen that the tension between D and  $^4\text{He}$  (or between the baryon density and  $^4\text{He}$ ) can be relieved by either of two variations of the standard model (slower than standard early expansion rate; nonzero chemical potential for the electron neutrino). However, in neither of these cases does the BBN-predicted  $^7\text{Li}$  abundance move any closer to that inferred from the observations.

In the current, data-rich era of cosmological research, BBN continues to play an important

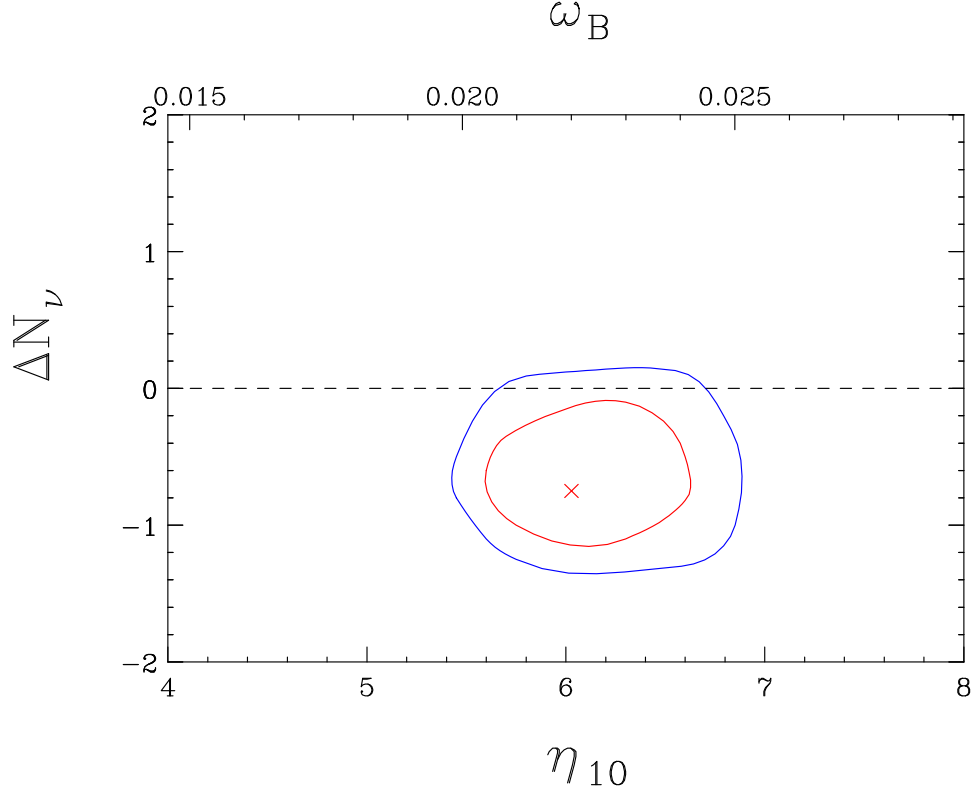


Fig. 1.14. The 1- and 2- $\sigma$  contours in the  $\eta - \Delta N_\nu$  plane for the joint BBN – CBR (WMAP) fit (Barger et al. 2003a).

role. The spectacular agreement in the baryon density inferred from processes occurring at widely separated epochs confirms the general features of the standard models of cosmology and particle physics. The tensions with  $^4\text{He}$  and  $^7\text{Li}$  provide challenges, and opportunities, to cosmology, to astrophysics, and to particle physics. To outline these challenges and opportunities, let us consider each of the light nuclides in turn.

For deuterium the agreement between SBBN and non-BBN determinations is perfect. This may be surprising given the unexpectedly large dispersion among the handful of extant D abundance determinations at high redshifts and low metallicities. Here, the challenge is to observers and theorists. Clearly more data are called for. Perhaps new data will reduce the dispersion. In that case it can be anticipated that the SBBN-predicted baryon density will approach the accuracy of that currently available from non-BBN data. On the other hand, newer data may support the dispersion, suggesting unexpectedly large variations in the D abundance at evolutionary times earlier than expected (Jedamzik & Fuller 1997). Perhaps there is more to be learned about early chemical evolution.

From studies of  $^3\text{He}$  in Galactic H II regions (Balser et al. 1997; Bania et al. 2002) it appears that in the course of Galactic chemical evolution there has been a very delicate balance between post-BBN production and destruction. If either had dominated, a gradient



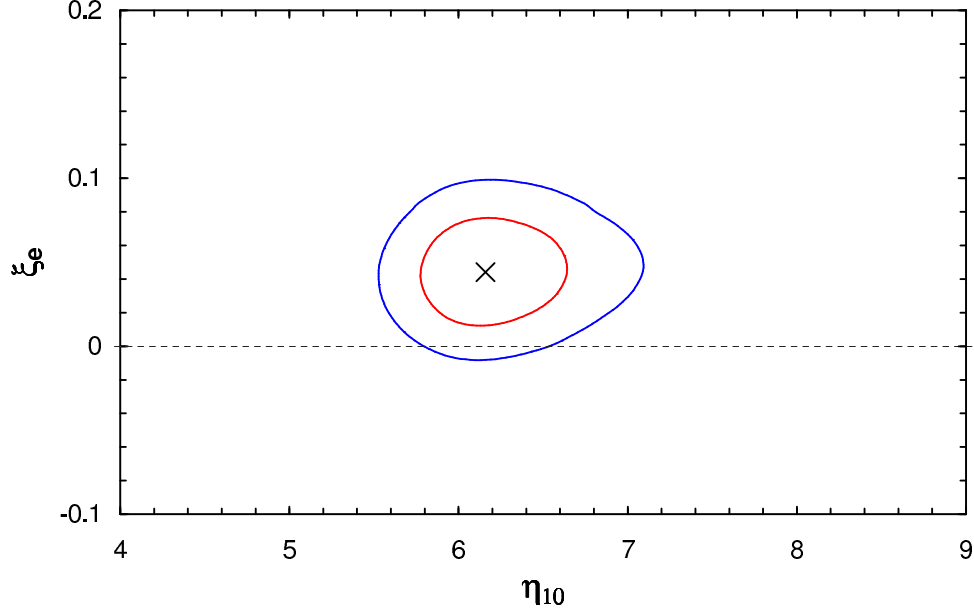


Fig. 1.15. The 1-, 2-, and 3- $\sigma$  contours in the  $\eta$ - $\xi_e$  plane for BBN ( $N_\nu = 3$ ) and the adopted D and  $^4\text{He}$  abundances (Barger et al. 2003b).

of the  $^3\text{He}$  abundance with galactocentric distance should have been seen in the data (see Romano et al. 2004, and references therein). So far, none is. Clearly, more data and a better understanding of the lower mass stars, which should dominate the production and destruction of  $^3\text{He}$ , would be of value.

The very precise value of the baryon density inferred either from D and SBBN or from non-BBN data, coupled with the very weak dependence of the SBBN abundance of  $^4\text{He}$  on the baryon density, leads to a very precise prediction of its primordial mass fraction. Although there exists a very large data set of  $^4\text{He}$  abundance determinations, the observational situation is confused at present. It seems clear that while new data would be valuable, quality is much more important than quantity. Data that can help resolve various corrections for temperature, for temperature and density fluctuations, for ionization corrections, would be of greater value than merely collecting more data that are incapable of addressing these issues. Because of the very large data set(s), the *statistical* uncertainty in the derived primordial mass fraction is very small,  $\sigma_{Y_p} \approx 0.002 - 0.003$ , while uncertain systematic corrections are much larger  $\gtrsim 0.005$ . At this point it is systematics, not statistics that dominate the uncertainty in the primordial helium abundance. In this context it is worth considering non-emission line observations that might provide an independent abundance determination. Just such an alternative, the so-called R-parameter method using globular cluster stars was proposed long ago by Iben (1968) and by Iben & Faulkner (1968). It too has many systematic uncertainties associated with its application, but they are different from those for the emission-line studies. Very recently, Cassisi, Salaris, & Irwin (2003), using new stellar models and nuclear reactions rates, along with better data, find  $Y_p = 0.243 \pm 0.006$ . This

*G. Steigman*

is in much better agreement with the expected value (within  $\lesssim 1\sigma$ ) and should stimulate further investigations.

The apparent conflict between the predicted and observed abundances of  ${}^7\text{Li}$ , if not simply traceable to the statistical and systematic uncertainties, suggests a gap in our understanding of the structure and evolution of the very old, metal-poor, halo stars. It would appear from the comparison between the predicted and observed abundances that lithium may have been depleted or diluted from the surfaces of these stars by  $\sim 0.2\text{--}0.4$  dex. Although a variety of mechanisms for depletion/dilution exist, the challenge is to account for such a large reduction without at the same time producing a large dispersion around the Spite plateau.

The wealth of observational data accumulated over the last decade or more have propelled the study of cosmology from youth to maturity. BBN has played, and continues to play, a central role in this process. There have been many successes, but much remains to be done. Whether the resolution of the current challenges are observational or theoretical, the future is bright.

**Acknowledgements.** I am grateful to all the colleagues with whom I have worked, in the past as well as at present, for all I have learned from them; I thank them all. Many of the quantitative results (and figures) presented here are from recent collaborations with V. Barger, J. P. Kneller, J. Linsky, D. Marfatia, K. A. Olive, R. J. Scherrer, S. M. Viegas, and T. P. Walker. I thank V. V. Smith for permission to use Figure 1.9. My research is supported at OSU by the DOE through grant DE-FG02-91ER40690.

## References

- Allende-Prieto, C., Lambert, D. L., & Asplund, M. 2001, *ApJ*, 556, L63  
Balser, D., Bania, T., Rood, R. T., & Wilson, T. 1997, *ApJ*, 483, 320  
Bania, T., Rood, R. T., & Balser, D. 2002, *Nature*, 415, 54  
Barger, V., Kneller, J. P., Lee, H.-S., Marfatia, D., & Steigman, G. 2003a, *Phys. Lett. B*, 566, 8  
Barger, V., Kneller, J. P., Marfatia, D., Langacker, P., & Steigman, G. 2003b, *Phys. Lett. B*, 569, 123  
Bennett, C. L., et al. 2003, *ApJS*, 148, 1  
Binetruy, P., Deffayet, C., Ellwanger, U., & Langlois, D. 2000, *Phys. Lett. B*, 477, 285  
Bonifacio, P., et al. 2002, *A&A*, 390, 91  
Bonifacio, P., & Molaro, P. 1997, *MNRAS*, 285, 847  
Bonifacio, P., Molaro, P., & Pasquini, L. 1997, *MNRAS*, 292, L1  
Bratt, J. D., Gault, A. C., Scherrer, R. J., & Walker, T. P. 2002, *Phys. Lett. B*, 546, 19  
Burles, S., Nollett, K. M., & Turner, M. S. 2001, *Phys. Rev. D*, 63, 063512  
Burles, S., & Tytler, D. 1998a, *ApJ*, 499, 699  
———. 1998b, *ApJ*, 507, 732  
Cassisi, S., Salaris, M., & Irwin, A. W. 2003, *ApJ*, 588, 862  
Chaboyer, B. C., Deliyannis, C. P., Demarque, P., Pinsonneault, M. H., & Sarajedini, A. 1992, *ApJ*, 388, 372  
Chiappini, C., Renda, A., & Matteucci, F. 2002, *A&A*, 395, 789  
Cline, J. M., Grojean, C., & Servant, G. 1999, *Phys. Rev. Lett.*, 83, 4245  
Crotty, P., Lesgourgues, J., & Pastor, S. 2003, *Phys. Rev. D*, 67, 123005  
Dearborn, D. S. P., Schramm, D. N., & Steigman, G. 1986, *ApJ*, 203, 35  
Dearborn, D. S. P., Steigman, G., & Tosi, M. 1996, *ApJ*, 465, 887 (erratum: *ApJ*, 473, 570)  
D’Odorico, S., Dessauges-Zavadsky, M., & Molaro, P. 2001, *A&A*, 368, L21  
Epstein, R., Lattimer, J., & Schramm, D. N. 1976, *Nature*, 263, 198  
Galli, D., Stanghellini, L., Tosi, M., & Palla, F. 1997, *ApJ*, 477, 218  
Geiss, J., & Gloeckler, G. 1998, *Space Sci. Rev.*, 84, 239  
Gruenewald, R., Steigman, G., & Viegas, S. M. 2002, *ApJ*, 567, 931  
Hannestad, S. 2003, *JCAP*, 5, 4  
Iben, I., Jr. 1967, *ApJ*, 147, 624  
———. 1968, *Nature*, 220, 143

*G. Steigman*

- Iben, I., Jr., & Faulkner, J. 1968, *ApJ*, 153, 101
- Izotov, Y. I., & Thuan, T. X. 1998, *ApJ*, 500, 188
- Izotov, Y. I., Thuan, T. X., & Lipovetsky, V. A. 1997, *ApJS*, 108, 1
- Jedamzik, K., & Fuller, G. 1997, *ApJ*, 483, 560
- Kang, H.-S., & Steigman, G. 1992, *Nucl. Phys. B*, 372, 494
- Kirkman, D., Tytler, D., Suzuki, N., O'Meara, J. M., & Lubin, D. 2004, *ApJS*, submitted (astro-ph/0302006)
- Kneller, J. P., Scherrer, R. J., Steigman, G., & Walker, T. P. 2001, *Phys. Rev. D*, 64, 123506
- Kneller, J. P., & Steigman, G. 2003, *Phys. Rev. D*, 67, 063501
- Levshakov, S. A., Dessauges-Zavadsky, M., D'Odorico, S., & Molaro, P. 2002, *ApJ*, 565, 696 [see also the preprint(s) astro-ph/0105529 (v1 & v2)]
- Levshakov, S. A., Kegel W. H., & Takahara, F. 1998a, *ApJ*, 499, L1
- . 1998b, *A&A*, 336, L29
- . 1999, *MNRAS*, 302, 707
- Linsky, J. L., & Wood, B. E. 2000, in *IAU Symp. 198, The Light Elements and Their Evolution*, ed. L. da Silva, M. Spite, & J. R. Medeiros (San Francisco: ASP), 141
- Olive, K. A., & Steigman, G. 1995, *ApJS*, 97, 49
- Olive, K. A., Skillman, E., & Steigman, G. 1997, *ApJ*, 483, 788
- Olive, K. A., Steigman, G., & Walker, T. P. 2000, *Phys. Rep.*, 333, 389
- O'Meara, J. M., Tytler, D., Kirkman, D., Suzuki, N., Prochaska, J. X., Lubin, D., & Wolfe, A. M. 2001, *ApJ*, 552, 718
- Palla, F., Bachiller, R., Stanghellini, L., Tosi, M., & Galli, D. 2000, *A&A*, 355, 69
- Peimbert, A., Peimbert, M., & Luridiana, V., 2002, *ApJ*, 565, 668
- Peimbert, M., Peimbert, A., & Ruiz, M. T. 2000, *ApJ*, 541, 688
- Pettini, M., & Bowen, D. V. 2001, *ApJ*, 560, 41
- Pierpaoli, E. 2003, *MNRAS*, 342, L63
- Pinsonneault, M. H., Steigman, G., Walker, T. P., & Narayanan, V. K. 2002, *ApJ*, 574, 398 (PSWN)
- Pinsonneault, M. H., Walker, T. P., Steigman, G., & Narayanan, V. K. 1999, *ApJ*, 527, 180
- Randall, L. & Sundrum, R. 1999a, *Phys. Rev. Lett.*, 83, 3370
- . 1999b, *Phys. Rev. Lett.*, 83, 4690
- Romano, D., Tosi, M., Matteucci, F., & Chiappini, C. 2004, *MNRAS*, in press
- Rood, R. T. 1972, *ApJ*, 177, 681
- Rood, R. T., Bania, T. M., Balser, D. S., & Wilson, T. L. 1998, *Space Sci. Rev.*, 84, 185
- Rood, R. T., Steigman, G., & Tinsley, B. M. 1976, *ApJ*, 207, L57
- Ryan, S. G., Beers, T. C., Olive, K. A., Fields, B. D., & Norris, J. E. 2000, *ApJ*, 530, L57
- Ryan, S. G., Norris, J. E., & Beers, T. C. 1999, *ApJ*, 523, 654
- Sackmann, I.-J., & Boothroyd, A. I. 1999a, *ApJ*, 510, 217
- . 1999b, *ApJ*, 510, 232
- Salaris, M., & Weiss, A. 2002, *A&A*, 388, 492
- Sauer, D., & Jedamzik, K. 2002, *A&A*, 381, 361
- Spergel, D. N., et al. 2003, *ApJS*, 148, 175
- Spite, M., & Spite, F. 1982, *Nature*, 297, 483
- Steigman, G. 2004, in *The Dark Universe: Matter, Energy, and Gravity*, ed. M. Livio (Baltimore: STScI), in press (astro-ph/0107222)
- Steigman, G., Schramm, D. N., & Gunn, J. E. 1977, *Phys. Lett. B*, 66, 202
- Steigman, G., Viegas, S. M., & Gruenwald, R. 1997, *ApJ*, 490, 187
- Theado, S., & Vauclair, S. 2001, *A&A*, 375, 70
- Thorburn, J. A. 1994, 421, 318
- Vassiliadis, E., & Wood, P. R. 1993, *ApJ*, 413, 641
- Viegas, S. M., Gruenwald, R., & Steigman, G. 2000, *ApJ*, 531, 813